의학박사 학위논문

Enhanced efficacy of radiation therapy by the overexpression of chromatin remodeling factor BRG1-bromodomain

BRG1-브로모도메인 과발현을 이용한 방사선 치료 효과 증진

2016 년 08 월

서울대학교 대학원

의과학과 의과학전공

나 주 리

A thesis for the Degree of Doctor of Philosophy

BRG1-브로모도메인 과발현을 이용한 방사선 치료 효과 증진

Enhanced efficacy of radiation therapy by the overexpression of chromatin remodeling factor BRG1-bromodomain

August, 2016

The Department of Biomedical Sciences,
Seoul National University
College of Medicine
Juri Na

Enhanced efficacy of radiation therapy by the overexpression of chromatin remodeling factor BRG1−bromodomain

by
Juri Na

A thesis submitted to the Department of Biomedical Sciences in partial fulfillment of the requirements for the Doctor Degree of Philosophy in Biomedical Sciences at Seoul National University College of Medicine

August, 2016

Approved by Thesis Committee:

Professor _____Chairman
Professor _____Vice chairman
Professor _____
Professor _____
Professor _____

ABSTRACT

Objectives: While radiation therapy is widely used to treat some types of cancer, cancer cells easily develop radiation resistance resulting in poor prognosis. Therefore, radiation sensitization is useful for the efficient treatment of cancer cells. Brahma-related gene 1 (BRG1), the catalytic subunit of the SWI/SNF chromatin-remodeling complex, is involved in DNA double-strand break (DSB) repairs. Overexpression of the BRG1 bromodomain (BRD) site and consequent competitive inhibition results in an inability to induce DNA repair, leading to the accumulation of DSBs. This study aims to improve the therapeutic effect of radiation through overexpression of the BRG1 BRD, resulting in increased competitive inhibition and inefficient DSB repair.

Methods: For visualizing tumor growth, luciferase expressing tumor cell lines were established. To monitor the therapeutic effect of external beam radiation, HT29 human colon cancer cells were used. Retroviral pMX-BRG1-BRD vectors were transfected into HT29 cells to establish a BRD over-expressing cell line, with both low and high (1.48-times higher) copy

numbers. The cells were irradiated using a ^{137}Cs irradiator (IBL 437C) at 9 Gy. The radio-sensitizing effects were measured through a clonogenic assay and analysis of phosphorylated H2AX foci. Tumor cells that were subcutaneously implanted into Balb/c nude mice, imaged by an *in vivo* imaging system, and measured using calipers.

Results: The survival rates of irradiated (9 Gy) cells expressing low and high levels of BRD were 51.4% and 2.2%, respectively, compared to BRD non-transduced HT29 cells. The fluorescence intensity of phosphorylated H2AX foci for cells with low (2.9 times) and high (9.9 times) BRD levels were higher than that in HT29-luc cells. Tumor growth was reduced corresponding to higher BRG1-BRD expression levels *in vivo;* bioluminescence signals of low and high overexpression of BRG1-BRD in tumors at 28 days after ionizing radiation were found to be 40.77 % ($p = 0.048$) and 7.37% ($p = 0.018$) higher, respectively, than that in control tumors.

Conclusion: The radiation-sensitizing effect of BRG1-BRD overexpression in human colon cancer cells was successfully demonstrated using molecular imaging techniques.

Keywords: BRG1-Bromodomain, radiosensitizer, effective radiation therapy, competitive inhibition, gene overexpression, X-ray therapy

Student number: 2010-21902

CONTENTS

LIST OF TABLES AND FIGURES

LIST OF ABBREVIATIONS

BRG1, Brahma-related gene 1

BRD, Bromodomain

DSB, double strand breaks

SWI/SNF complex, SWItch/Sucrose Non-Fermentable complex

RT-PCR, Reverse Transcription-Polymerase Chain Reaction

FBS, Fetal Bovine Serum

IVIS, In Vivo Imaging System

ATM, Ataxia Telangiectasia Mutated

LINAC, Linear Accelerator

TUNEL, Terminal deoxynucleotidyl transferase dUTP nick end labeling

ABC, Avidin-biotin complex

DAB, 3,3'-Diaminobenzidine

HIER, heat induced epitope retrieval

INTRODUCTION

Along with surgery and chemotherapy, radiation is an important method for treating malignant tumors. At least, 50% of various cancer patients receive radiation therapy as standard treatment [1−4]. Radiation therapy uses high−energy radiation to shrink tumors and to kill cancer cells [5, 6]. High energy X−rays, beta rays, and charged particles are the types of radiation that are used for cancer treatment. Several types of radiation therapy exist including external radiation therapy, internal radiation therapy, and brachytherapy. External radiation therapy uses radiation delivered by a machine outside the body whereas internal radiation therapy uses radioactive substances, such as radioactive iodine, that travel in the blood and accumulate in the tumor to kill cancer cells. Brachytherapy involves the placement of radioactive material in the body near the cancer cells. External radiotherapy is the most common form of radiotherapy. An external source of radiation is targeted to the tumor located in the body. Normally, cancer patients receive external radiotherapy for five days a week in split doses for 4 weeks to kill cancer cells specifically while protecting normal cells [7].

However, normal cells as well as cancer cells begin to repair themselves from the damage induced by external radiotherapy. Hence, some cancers are not fully treated with external radiotherapy owing to radioresistance.

The most vulnerable material in the cell is DNA, because it cannot be replaced. DNA damage can occur owing to spontaneous base hydrolysis and during natural stress such as inflammation and radiation [8, 9]. Radiation therapy kills cancer cells by damaging their DNA [5, 6], either directly or by creating charged particles within the cells that in turn damage the DNA. Radiotherapy sometimes triggers radiation resistance in cancer cells [10].

Radiosensitizers have been developed to avoid the acquisition of radio-resistance in cancer cells. Here, a new method for radio-sensitization has been investigated, which targets the inhibition of DNA DSB repair mechanisms. Although both single- (SSBs) and double-strand breaks (DSBs) in DNA are observed, DSBs are primarily induced by base damage, reactive oxygen species, and ionizing radiation [11]. SSBs are discontinuities in one strand of the DNA double helix [12]. SSBs can occur directly by the disintegration of oxidized sugars or indirectly during DNA base-

excision repair of oxidized bases, abasic sites, or bases that are damaged or altered in other ways [13–15]. Around ~105 ionization events equivalent to ~1,000–2,000 SSBs or 40 DSBs per cell are induced after irradiation with 1 Gy X–rays [16]. Brahma–related gene 1 (BRG1), a chromatin remodeling enzyme, facilitates DSB repairs by stimulating γ–H2AX formation. This BRG1 function requires the binding of BRG1 to acetylated histone H3 on γ–H2AX–containing nucleosomes through its bromodomain (BRD), a protein module that specifically recognizes acetyl–Lys moieties [17]. BRG1–BRD, when ectopically expressed in cells, functions as a dominant negative inhibitor of BRG1 activity [18], resulting in inefficient DSB repair. Thus, we considered the concept that blocking γ–H2AX and DSB repair by ectopic expression of BRG1–BRD could help induce apoptosis after radiation therapy. Histone H2AX phosphorylation is part of the major DNA damage signaling network that is activated by the presence of a critical lesion, the DNA double–strand break [19–22]. For the DSB repair and damage response, both histone modification and ATP–dependent chromatin remodeling are important. The highly ordered chromatin, which

has a compact genome structure, controls cellular mechanisms by allowing regulatory proteins to access their target DNA [23]. DSBs are triggered by any damages to DNA, and Ataxia telangiectasia mutated (ATM) initiates the phosphorylation of serine 139 (S139ph) and establishes γ-H2AX on the chromatin around a DSB. γ-H2AX then triggers the acetylation of H3 lysine 14 which binds to the chromatin remodeling complex, SWI/SNF. The increased level of S139ph leads to further acetylation of H3 and accumulation of SWI/SNF at γ-H2AX nucleosomes. This acetylation eventually establishes high levels of γ-H2AX that are necessary for an efficient DSB response [24]. This kind of DNA self-repair mechanism helps malignant cells recover after radiation therapy. The chromatin remodeling factor SWI/SNF has several subunits, one of which is BRG1. The BRG1-BRD binds to acetylated H3, which has a cooperative action with S139ph. If BRG1-BRD were inhibited from binding to acetylated H3, DNA repair would also be inhibited. Thus, by blocking the DNA self-repair mechanism through overexpression of the BRG1-BRD competitor, acetylation of H3 lysine 14 and phosphorylation of serine 139 can occur [25].

Several radiosensitizers have been developed, and most of these radiosensitizers are constructed as chemical drugs such as genistein and curcumin [26]. However, this study aims to demonstrate the radiation-sensitizing effect of gene modification through BRG1-BRD overexpression in human colon cancer cells and by visualizing the damage using molecular imaging.

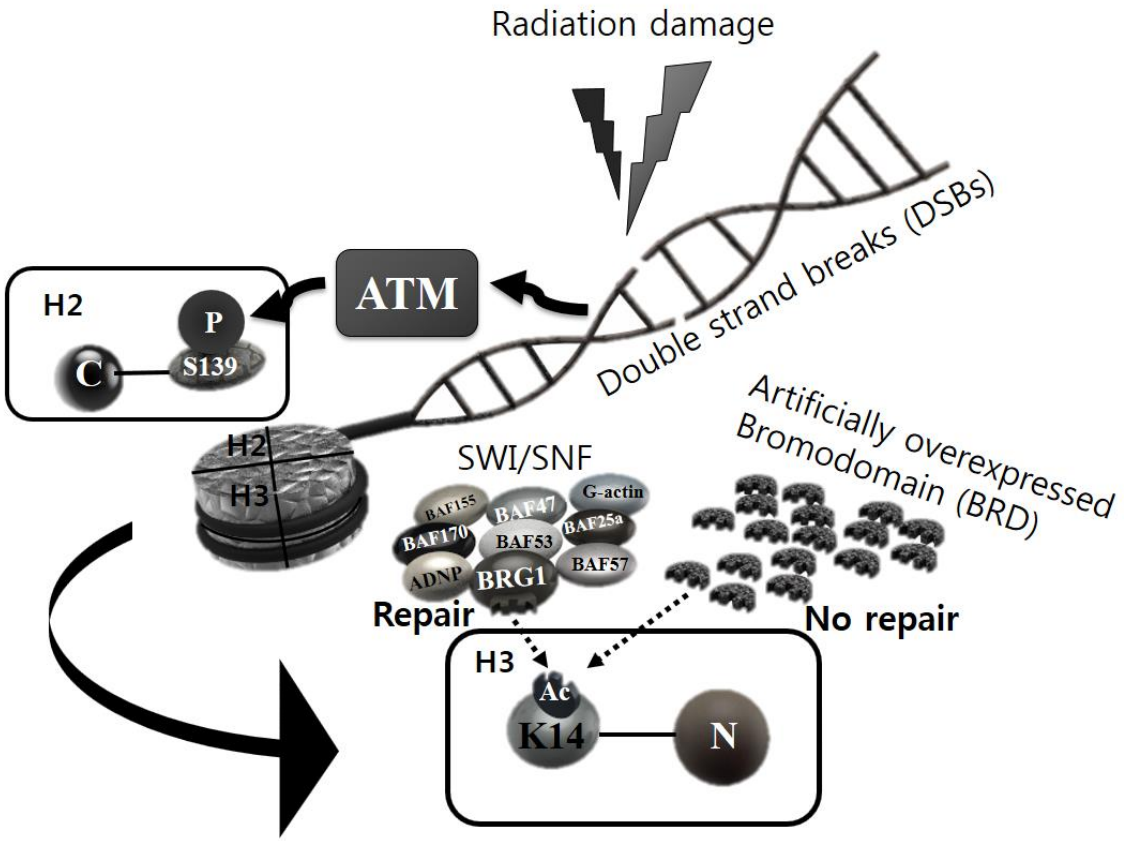
Radiation damage
ATM
H2
P
C
S139
Double strand breaks (DSBs)
H2
H3
SWI/SNF
BAF155
BAF47
G-actin
BAF170
BAF53
BAF25a
ADNP
BRG1
BAF57
Artificially overexpressed
Bromodomain (BRD)
Repair
No repair
H3
Ac
K14
N

Figure 1. The radiosensitizing mechanism of BRG1-BRD overexpression.

Novel crosstalk between a chromatin-remodeling complex and two different types of histone modifications for DNA repair has been reported [24]. There is a cooperative activation loop between SWI/SNF, γ-H2AX, and H3 acetylation for DSB repair. DNA DSBs can be induced when cells are exposed to an energy producing external environment. These DSBs activate ATM and they initiate the phosphorylation of serine 139 and resulting in low levels of γ-H2AX on the chromatin around a DSB. This γ-H2AX triggers the acetylation of H3 within the nucleosomes. SWI/SNF then binds to γ-H2AX nucleosomes by interacting with acetylated H3 using the BRD of BRG1. This positive feedback loop between SWI/SNF, S139ph, and H3 acetylation eventually establishes high levels of γ-H2AX for an efficient DSB response [24]. The unlimited overexpression of artificial BRG1-BRD, results in stochastic binding to acetylated H3, which blocks this DSB repair mechanism.

MATERIALS AND METHODS

1. Cell culture and reagents

HT29 human colon cancer cells were maintained in McCoy's medium (WelGene Inc., Seoul, Korea) containing 10% heat-inactivated fetal bovine serum (Gibco, NY, USA) and 1% penicillin/streptomycin at 37°C and 5% CO_2. HCT116 human colon cancer cells were maintained in RPMI medium (WelGene Inc., Seoul, Korea) containing 10% heat-inactivated fetal bovine serum (Gibco, NY, USA) and 1% penicillin/streptomycin at 37°C and 5% CO_2.

For visualizing the cells, pCMV-luciferase retro-viral vector was transfected into the HT29 cells using pCMV-luciferase viruses harvested from the 293FT cell line and Lipofectamine 2000 (Invitrogen, CA, USA) including gag, pol, env. Luciferase-expressing HT29 cells (HT29-luc) were clonally selected in 96 well plates and the luciferase activity of these selected cells was confirmed using the *in vivo* imaging system (IVIS) 100 (Caliper life Sciences, MA, USA). For BRG1-BRD overexpression, BRG1-BRD with a myc-tag to detect the recombinant protein

expression was transfected into HT29-luc cells for 2 days. The simplified vector map expressing the BRG1-BRD is presented in Figure 2(B). The transfection efficiency of the cells was evaluated to measure the photon flux signals using IVIS 100 and real time PCR.

2. Cell irradiation

Cells plated flasks were prepared one day before irradiation. Irradiations were conducted using a γ-ray irradiator (CIS IBL 473C) at a dose of 3, 6, and 9 Gy at room temperature.

3. Clonogenic assay

In this study, 100 or 200 HT29-luc, HT29-luc-BRD(L), and HT29-luc-BRD(H) cells were plated in 6-well plates (Nunc, Leuven, Belgium) in triplicate wells with McCoy's medium supplemented with 10% fetal bovine serum and 1% penicillin/streptomycin. After 24 h, ^{125}Cs γ-ray ionizing radiation of 3, 6, and 9 Gy was administered to the cells using a γ-ray irradiator (CIS IBL 473C). After 2-3 weeks, colonies of the irradiated cells were stained with a crystal violet (Sigma Aldrich,

MO, USA) solution made from 0.5 g crystal violet, 25 ml of 40% formaldehyde, 50 ml ethanol, and 175 ml DW. The colonies were counted and the mean and standard deviation were calculated.

4. Western blotting

BRG1-BRD-overexpressing HT29-luc cells were lysed in RIPA buffer (Sigma-Aldrich, MO, USA) containing protease inhibitor cocktail tablets (Roche, Cher, France). The concentration of the extracted protein was analyzed using the bicinchoninic acid assay (BCA) assay (Pierce, IL, USA). The proteins (30 μg) proteins were separated by SDS-PAGE under reducing conditions and were transferred onto a PVDF membrane (Millipore, Molsheim, France). After blocking with 5% skim milk for 1 h, the membranes were incubated with anti-myc-tag mouse monoclonal antibody (Cell Signaling, MA, USA) followed by incubation with horseradish peroxidase conjugated anti-mouse secondary antibody (Cell Signaling, MA, USA) for 1 h at room temperature. β-actin (Sigma-Aldrich, MO, USA) was used as the loading control. Immunoreactive bands were detected with enhanced chemiluminescence reagents (Roche, Cher, France) using the LAS-3000 Imaging System (Fujifilm, CA, USA).

5. Quantitative real-time reverse transcription polymerase chain reaction (qPCR)

Total RNA was extracted from cultured cells using Trizol (Qiagen, CA, USA) as per the manufacturer's protocol. RNA was quantified spectroscopically (ND-1000 Spectrophotometer, NanoDrop, DE, USA). RNA (1 μg) was subjected to reverse transcription in a total volume of 20 μl. Following 10-fold dilution with water, 2 μl of cDNA was used in a 20 μl qPCR reaction. PCR was performed in triplicate using cDNA synthesized from total RNA with gene-specific primers according to the TaqMan RT master mix (PE Applied Biosystems, CA, USA). Reverse transcriptase reactions contained 1 μg of RNA samples, 3 μl primers, 7 μl master mix (all purchased from RT master mix Applied Biosystems). The 15 μl reactions were incubated in an S-1000 Thermal Cycler (Bio-Rad, CA, USA) in 0.2 ml polypropylene reaction tubes for 30 min at 16°C, 30 min at 42°C, 5 min at 85°C and then held at 4°C. Real-time PCR was performed using an Applied Biosystems 7500 Sequence Detection system.

The 20 μl PCR mixture included 9 μl of RT product, 10 μl of 2× TaqMan gene expression master mix, and 1 μl each of primer and probe mix from the TaqMan gene expression assay protocol (PE Applied Biosystems). The reactions were incubated in a 96-well optical plate at 50°C for 2 min, 95°C for 10 min, followed by 40 cycles of 95°C for 15 s and 60°C for 10 min. The mRNA levels of the myc-tag were determined using the following primers: forward 5′-GGTAGATACGGCCGCAGAA-3′ and reverse 5′-CGGCCCCATTCAGATCCT-3′ designed with the FAM probe 5′-CTTCTGAGATGAGTTTTTG-3′ for fluorescence detection. Glyceraldehyde-3-phosphate dehydrogenase (GAPDH) was used as an internal control.

6. Doubling time

For this assay, 5×10^4 HT29-luc, HT29-luc-BRD(L), and HT29-luc-BRD(H) cells were plated on 6-well plates in triplicate and were harvested at 24 h, 48 h and 72 h. Cells stained with trypan blue were counted using a hemocytometer and the doubling time of the harvested cells was calculated, using an algorithm available in the GraphPad Prism software (GraphPad Software, CA, USA):

$TD = t \times lg2 / (lgNt - lgN0)$

where N0 is the number of cells seeded, Nt is the number of cells harvested, and t is the culture time in hours

7. Immunocytochemistry for γ-H2AX foci staining

For staining of γ-H2AX in response to double-strand DNA damage and apoptosis, HT29-luc, HT29-luc-BRD(L) and HT29-luc-BRD(H) cells were irradiated with ^{125}Cs γ-rays at 9 Gy and fixed in methanol for 5 minutes at −20°C. After blocking in normal goat serum (Vector Laboratories, Inc., CA, USA) for 30 minutes, the cells were incubated overnight with γ-H2AX antibody (Cell signaling, MA, USA) at 4°C, washed and stained with Alexa Fluor 555 goat anti-rabbit IgG (Invitrogen, CA, USA) for 1 h at room temperature. The cells were mounted with ProLong Gold antifade reagent containing DAPI (Life Technologies, NY, USA) and observed using confocal microscopy (Carl Zeiss, MA, USA).

8. Colon tumor xenografts in nude mice

All procedures involving animals were approved by the Institutional Animal Care and Use Committee at Seoul National University, Republic of Korea and were consistent with the Guide for the Care and Use of Laboratory Animals [27]. 5×10^5 HT29-luc, HT29-luc-BRD(L), and HT29-luc-BRD(H) cells were subcutaneously injected into the flanks of male BALB/c nu/nu mice (7 weeks) along with 40 μl of matrigel. After tumor growth, the mice were irradiated with 9 Gy of high energy X-rays on the tumor-injected dorsal part using a linear accelerator (LINAC). The tumor bearing mice received an intraperitoneal (i.p.) administration of luciferin (3 mg/mouse; Molecular Probes), and were anesthetized with isoflurane. Bioluminescence imaging was performed using an IVIS (IVIS100; Xenogen Corp., CA, USA).

9. Immunohistochemistry

Tissues were fixed in 10% neutral-buffered formalin, processed, and embedded in paraffin. The paraffin-embedded sections were cleared and heated in an oven (65°C) for an hour. Deparaffinization was performed with xylene, alcohol (from 100% to 70%), and washing in distilled water for 5 min each and in 0.5% H_2O_2 methanol for 30 min to completely remove the embedded

materials before immunostaining. Slides immersed in 10 mM sodium citrate at pH 6.0 were boiled in a microwave for heat induced epitope retrieval (HIER). After cooling the slides at RT, 0.5% Triton X-100 in PBS solution was used for rinsing for 5 min. Blocking of the sections was performed with normal goat serum diluted at 1:30 in PBS for 30 min and primary antibody binding was also performed using several antibodies overnight (anti-myc-tag, #2276, Cell Signaling; anti-Ki67, ab16667, Abcam; anti-γ-H2AX, #2577, Cell Signaling) at 4°C. Biotinylated secondary antibodies were incubated with the sections for an hour at RT and ABC complex binding was performed before staining with DAB and hematoxylin. TUNEL assay was performed according to the manufacturer's recommendation, #S7100 (Millipore, Molsheim, France).

10. cDNA microarray

For control and test RNAs, synthesis of target cRNA probes and hybridization were performed using Agilent's Low RNA Input Linear Amplification kit (Agilent Technology, CA, USA) according to the manufacturer's instructions. Briefly, each 1 μg of total RNA and T7 promoter primer were mixed and incubated

at 65°C for 10 min. The cDNA master mix (5X First strand buffer, 0.1 M DTT, 10 mM dNTP mix, RNase-Out, and MMLV-RT) was prepared and added to the reaction mixture. The samples were incubated at 40°C for 2 h and the RT and dsDNA synthesis reaction was terminated by incubating at 65°C for 15 min. The transcription master mix was prepared as per the manufacturer's protocol (4X Transcription buffer, 0.1 M DTT, NTP mix, 50% PEG, RNase-Out, Inorganic pyrophosphatase, T7-RNA polymerase, and Cyanine 3-CTP). Transcription of dsDNA was performed by adding the transcription master mix to the dsDNA reaction samples and incubating at 40°C for 2 h. The amplified and labeled cRNA was purified on the cRNA Cleanup Module (Agilent Technology, CA, USA) according to the manufacturer's protocol.

RESULTS

Establishment of BRG1-BRD overexpressing and luciferase expressing colon cancer cell line

The radiosensitivity of colon cancer cells was compared using a clonogenic assay comparing between HT29 and HCT116 cells after irradiation with ^{137}Cs γ-rays at 3, 6, and 9 Gy. We confirmed that the HT29 cell line was more resistant to radiation than the HCT116 cells (Figure 1(A)). The luciferase reporter vector and the pMX-BRG1-BRD vector (Figure 1(B)) were transfected into the radiation resistant HT29 cells. The luciferase transfected HT29 cells (HT29-luc) were used for overexpressing the BRG1-BRD gene and these BRG1-BRD overexpressing HT29-luc cells were subjected to clonal selection. Using western blotting, the myc-tag inserted into the plasmids was detected in the BRG1-BRD overexpressing HT29-luc cells (Figure 3). Five selected BRG1-BRD overexpressing HT29 clones are shown in Figure 3 with various transfection efficacies and the 3rd and 5th clonally selected cells showed low (L) and high (H) expression of BRG1-BRD,

respectively. The luciferase activities of the clonally selected candidates, the lane 3 and 5 HT29-luc cells, were increased following cell density (Figure 4(A)). The regions of interest (ROI) were calculated and are presented in Figure 4(B). The HT29-luc, HT29-luc-BRD (L), and HT29-luc-BRD (H) cells showed a non-significant (n.s.) growth rate through the luciferase assay even after gene transfection (Figure 4(C)). BRG1-BRD overexpression was demonstrated by Real-time PCR (Figure 5), and this result is in agreement with the western blotting result (Figure 3). This cell line establishment indicates that the luciferase and the BRG1-BRD genes were transfected into the HT29 cells without any effect on their proliferation rate. Additionally, each clonally selected cell line showed different transfection efficacy, allowing the establishment of HT29-luc-BRD(L) and HT29-luc BRD(H) cells for comparing their characteristics.

(A)

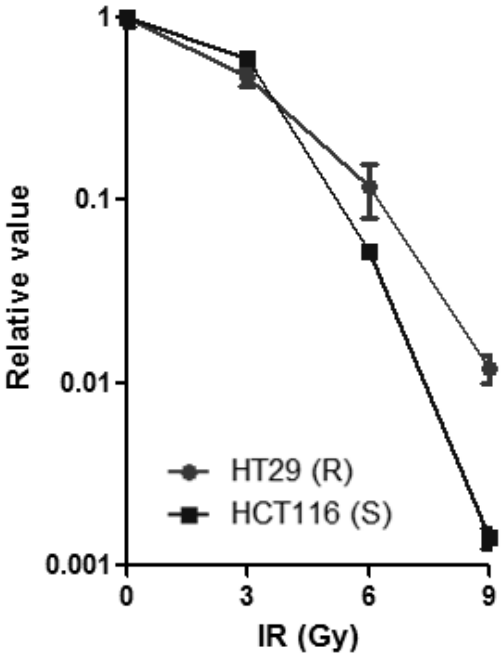
1
0.1
0.01
0.001
Relative value
HT29 (R)
HCT116 (S)
0
3
6
9
IR (Gy)

(B)

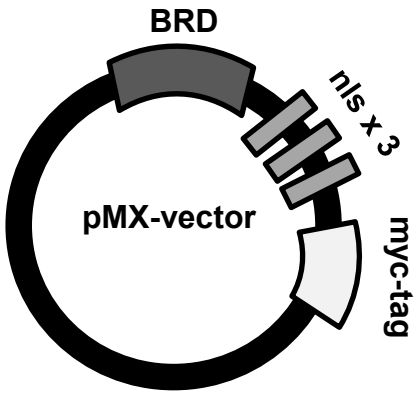
BRD
nls x 3
pMX-vector
myc-tag

Figure 2. Radio-resistant colon cancer cell line and the vector map for BRD overexpression.

(A) Two representative human colon cancer cell lines, HT29 and HCT116, were evaluated for their survival rate by a clonogenic assay. The HT29 cell line is more resistant than the HCT116 cell line, and so the HT29 cell line was used for BRD overexpression. (R) means radio-resistant; (S) means radio-sensitive. (B) The vector map for BRD overexpression is illustrated. The myc epitope tag is included to detect BRD overexpression. The epitope tags present usefulness for labeling and detection of proteins using immunoblotting, immunoprecipitation, and immunostaining techniques, and the myc epitope is also widely used to detect the expression of recombinant proteins in bacterial, yeast, insect, and mammalian cell systems [28]. Triplicated nuclear localization signals (nls × 3) are located between the BRD sequence and the myc-tag sequence.

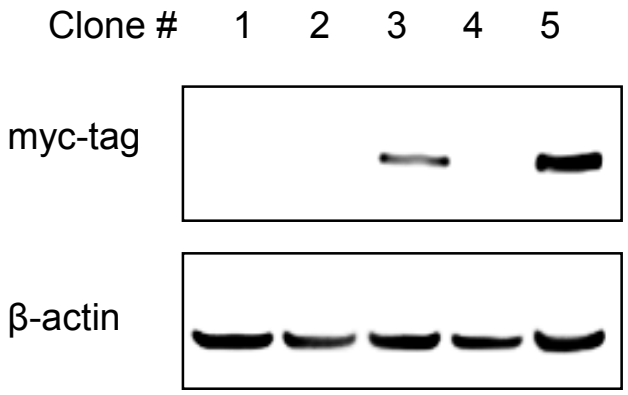

Figure 3. Establishment of BRD-overexpressing HT29 cell lines. Western blotting for the clonally selected HT29 cells after BRG1-BRD vector retroviral transfection showed different myc-tag protein levels indicating different levels of BRD overexpression. The low BRG1-BRD overexpressing HT29 cells, BRD(L), are shown in lane 3 and the high BRG1-BRD overexpressing HT29 cells, BRD(H), are shown in lane 5. The lane 5 shows 2.57 times stronger myc-expression than lane 3. The cells in line 5 are designated as BRD(H), indicating high expression of BRD; the cells in line 3 are designated as BRD(L), indicating low expression of BRD.

(A)

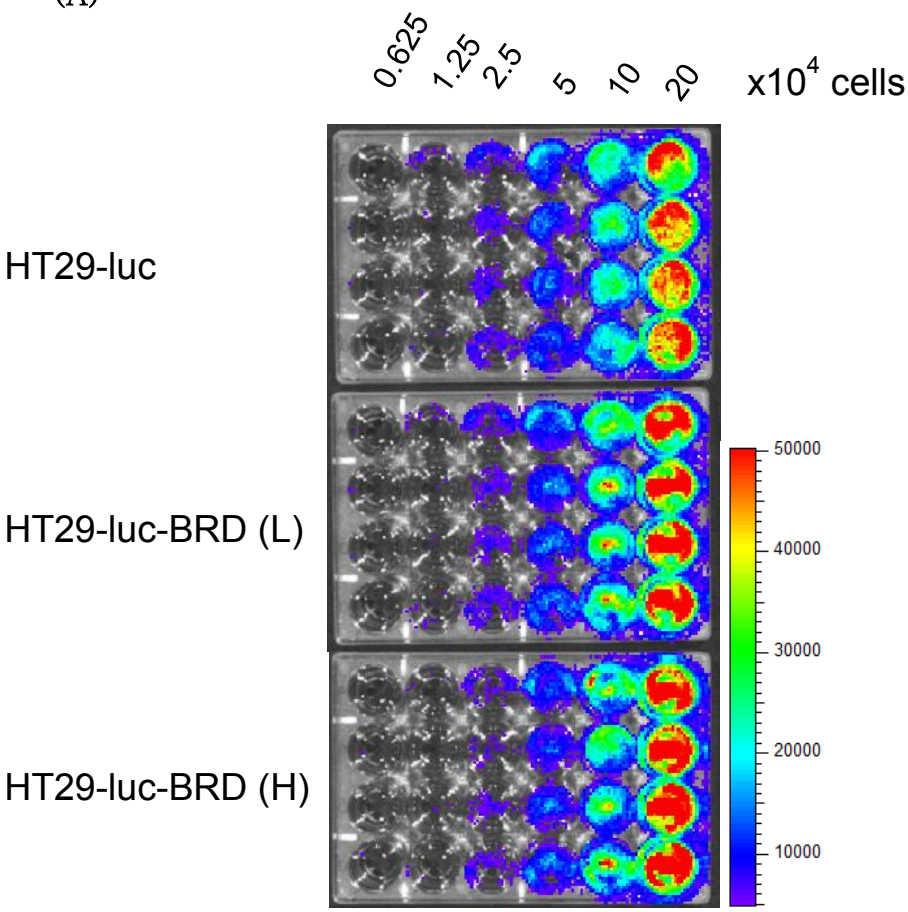
0.625
1.25
2.5
5
10
20
x10^4 cells
HT29-luc
HT29-luc-BRD (L)
HT29-luc-BRD (H)
50000
40000
30000
20000
10000

(B)

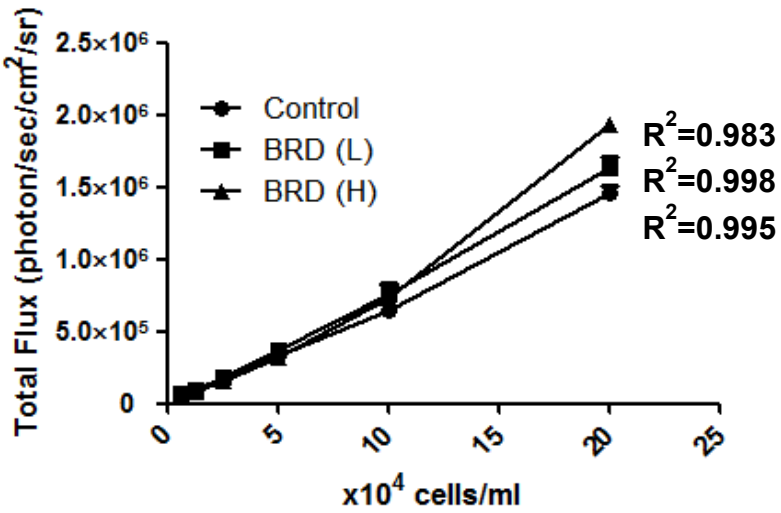
Total Flux (photon/sec/cm²/sr)
2.5×10⁶
2.0×10⁶
1.5×10⁶
1.0×10⁶
5.0×10⁵
0
Control
BRD (L)
BRD (H)
R²=0.983
R²=0.998
R²=0.995
0
5
10
15
20
25
x10⁴ cells/ml

(C)

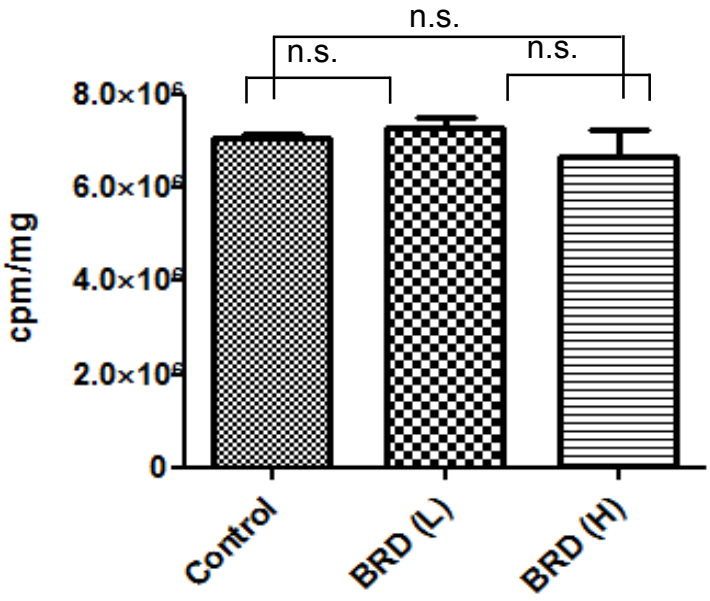

Figure 4. Establishment of luciferase expressing HT29 cell lines. (**A**) Bioluminescence images of luciferase gene transfected HT29 cells are as indicated. HT29-luc is designated as Control; HT29-luc-BRD(L) is designated as BRD(L); HT29-luc-BRD(H) is designated as BRD(H). (**B**) The total flux of cells increases depending on the plated cell numbers as shown. The R^2 values for these 3 cell lines are all higher than 0.98, indicating consistent luciferase expression. (**C**) To avoid the variation in plated cell numbers, a protein assay and luciferase assay were additionally performed for protein compensation. All three established cell lines express the luciferase gene without any significant differences.

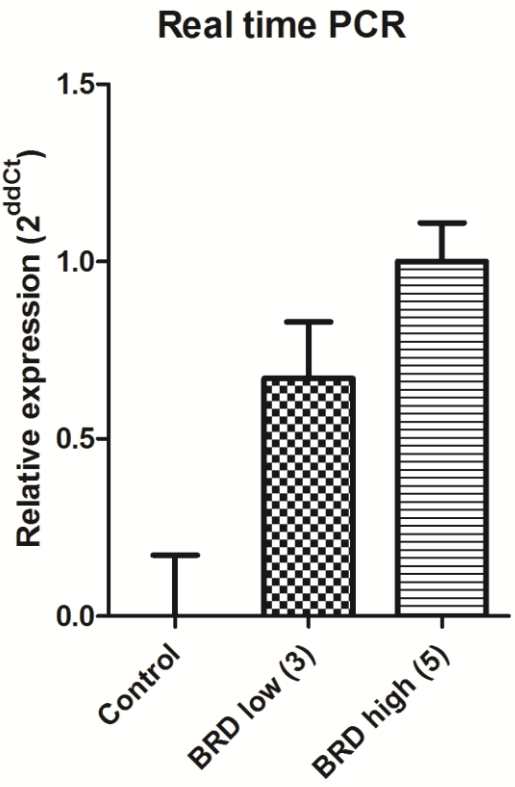

Figure 5. Monitoring BRD expression at the gene level in HT29-Luc cell lines.

Real time PCR analysis was performed on the BRD-overexpressing transfected HT29 cells after clonal selection. BRD(L) in lane 3 of Figure 3, and BRD(H) in line 5 of Figure 3 showed 1.49-fold BRD overexpression.

Radio-sensitizing effect of BRG1-BRD overexpression depends on the level of overexpression *in vitro*

We next evaluated whether BRG1-BRD overexpression levels regulate the extent of radio-sensitization in HT29 cells. The radio-sensitivity of HT29 cells was compared using a clonogenic assay between Control, BRD(L) and BRD(H) after irradiation with ^{137}Cs γ-rays at 3, 6, and 9 Gy (Figure 6). Once the BRG1-BRD gene was overexpressed in HT29 cells, the surviving fraction after irradiation with 9 Gy on the plates could only reach 2.16-51.44% of that in the control. Moreover, BRD(H) shows only 4.2% of the colonies in BRD(L) after irradiation with 9 Gy in the clonogenic assay (Figure 6(B)). To quantify the DNA damage repair abilities, immunocytochemistry of γ-H2AX foci was performed after the radiation treatment, and we could observe that permanent damages were retained (red color stained) in BRD(L) and BRD(H) at 72 h after 9 Gy radiation treatment (Figure 7). The initial kinetics of development of γ-H2AX over 4-8 h was similar for the control, BRD(L), and BRD(H). However, while the control cell line showed loss of γ-H2AX beginning about 8 h after the radiation treatment, BRD(L)

and BRD(H) cells continued to show increases in the expression of γ-H2AX. The percentage of γ-H2AX foci-stained cells was significantly higher in BRD(L) and BRD (H) (2.91 and 9.92-times more stained cells, respectively, against control at 72 h after radiation, Figure 7(B)). To evaluate the DNA strand breaks, DNA fragmentation after radiation treatment was assessed and we could observe that smeared DNA, which reflects the number of DNA breaks, was severe in the BRD(L) and BRD(H) cells (Figure 8). Thus, these findings suggest that BRG1-BRD overexpression enhances radio-sensitivity through poor DNA damage repair ability in the DSB DNA repair mechanism. Thus, higher expression of BRG1-BRD induces higher radio-sensitization in colon cancer cells.

(A)

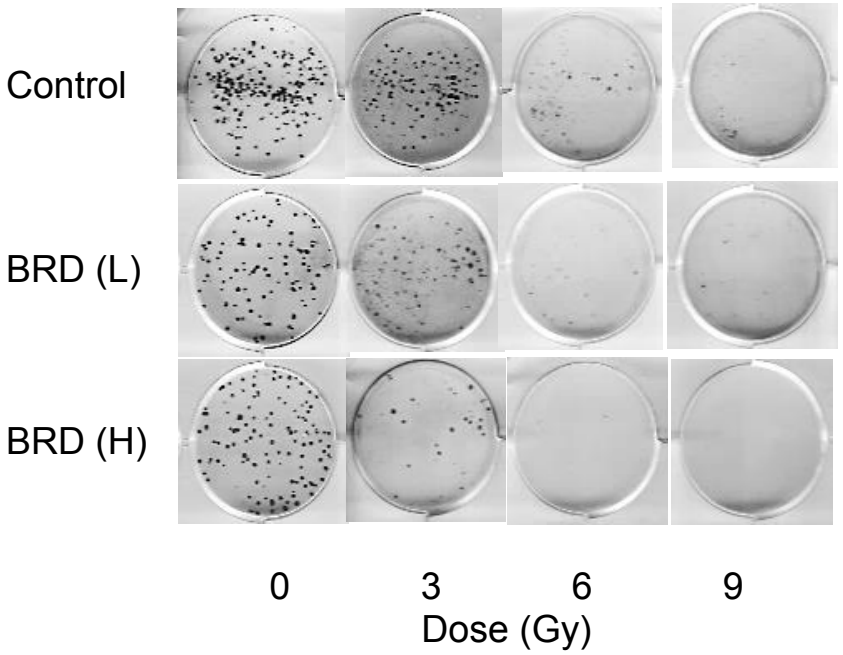
Control
BRD (L)
BRD (H)
0
3
6
9
Dose (Gy)

(B)

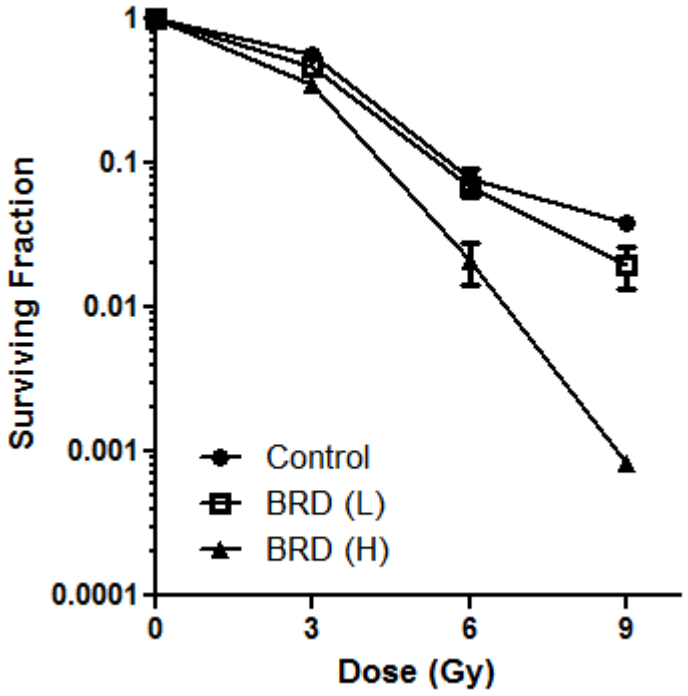
Surviving Fraction
1
0.1
0.01
0.001
0.0001
0
3
6
9
Dose (Gy)
Control
BRD (L)
BRD (H)

Figure 6. Cell survival rates with BRD overexpression after external radiation therapy.

The clonogenic assay detects all the cells that have retained the capacity for producing a large number of progeny after treatments that can cause cell reproductive death as a result of damage to chromosomes, apoptosis, and so on [29, 30]. (A) Control, BRD(L), and BRD(H) cells were plated in 6-well plates and irradiated with 3, 6, and 9 Gy by a ^{125}Cs γ-irradiator. Compared to the control cells, BRD(L) and BRD(H) cells show less colony formation after irradiation. (B) The cell survival rate after irradiation was calculated and graphed.

Control, filled circles; BRD(L), open squares; BRD(H), filled triangles.

(A)

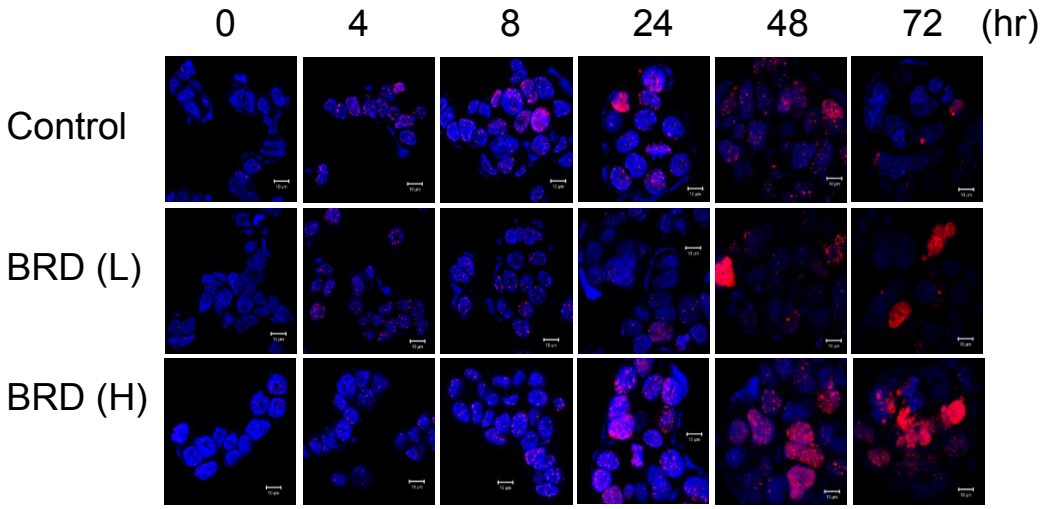
0
4
8
24
48
72
(hr)
Control
BRD (L)
BRD (H)

(B)

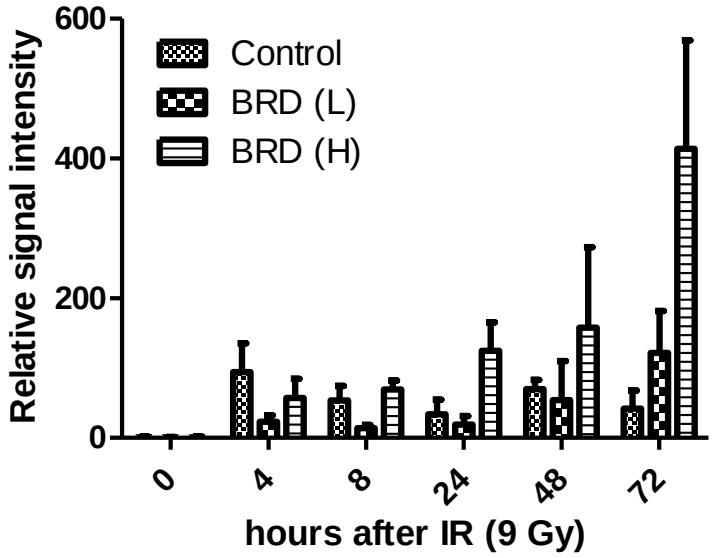
600
400
200
0
Relative signal intensity
Control
BRD (L)
BRD (H)
0
4
8
24
48
72
hours after IR (9 Gy)

Figure 7. Imaging DNA double strand breaks with BRD overexpression after external radiation therapy.

γ-H2AX expression is an early cellular response to the induction of DNA double-strand breaks (DSBs) and these are the most deleterious DNA lesions, which if left unrepaired, may have severe consequences on cell survival, as they lead to chromosomal aberrations, genomic instability, or cell death [31-33]. (**A**) Control, BRD(L), and BRD(H) cells were plated in 8-well chamber slides and irradiated with 3, 6, and 9 Gy by a ^{125}Cs γ-irradiator. Compared to the control cells, BRD(L), and BRD(H) cells show more γ-H2AX foci after irradiation. (**B**) γ-H2AX foci showing DNA DSBs after irradiation were calculated and graphed. Control, filled circles; BRD(L), open squares; BRD(H), filled triangles.

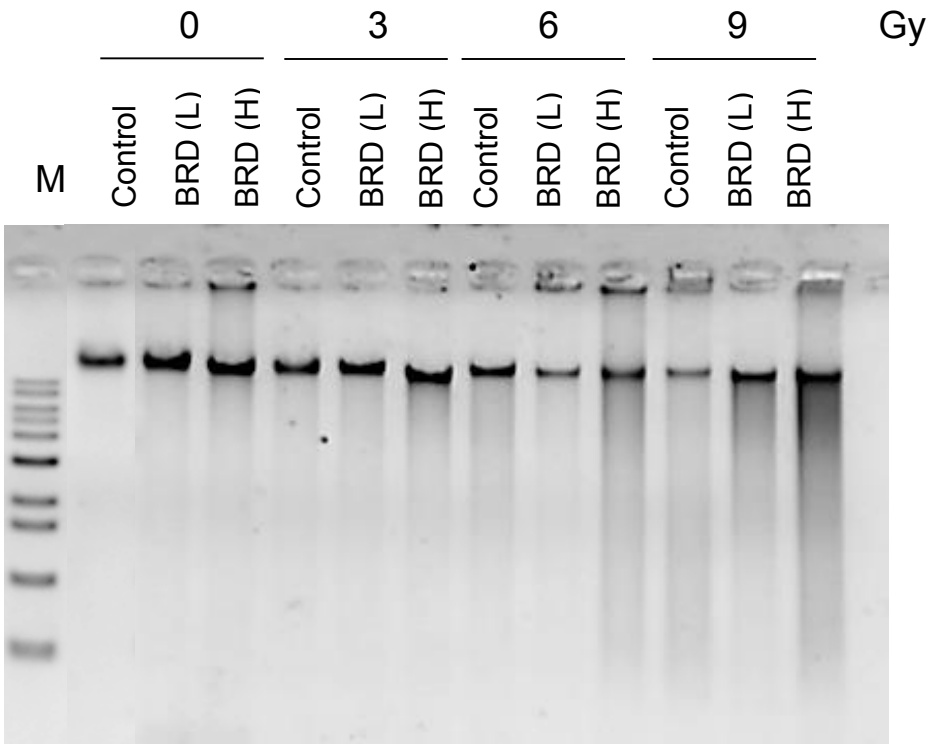

Figure 8. Identification of programmed cell death after exposure to radiation.

The existence of programmed cell death is inferred mainly from gel electrophoresis of a pooled DNA extract as programmed cell death is known to be associated with DNA fragmentation [34]. DNA analysis by 1.2% agarose gel electrophoresis of genomic DNA extracted from the control, BRD(L), and BRD(H) cell lines incubated for 2 weeks after irradiation.

Antitumor efficacy of radiation therapy with two levels of BRG1-BRD overexpression in an *in vivo* model of HT29

To evaluate the radio-sensitizing efficacy of BRG1-BRD overexpression in an *in vivo* model of colon cancer cells, we established an animal model of control, BRD(L) and BRD(H) tumors in Balb/c-nude mice by subcutaneous injection of these cells. Mice bearing tumors their right flank were irradiated with 9 Gy of high energy X-rays following the schedule shown in Figure 9. We first verified that our mouse model represents the radio-sensitizing effect depending on the BRG1-BRD expression level using an *in vivo* imaging system (IVIS) (Figure 9(B)) to observe the tumor proliferation and survival rate. The total flux (photon·sec^{-1}·cm^{-2}·sr^{-1}) was automatically measured by the Living Image software and ROI measurements show that the tumor sensitivity to radiation increased with increase in BRG1-BRD overexpression (Figure 9(C)). BRD(L) and BRD(H) implanted mice showed 40.80% and 7.38% proliferation compared to control cells. Moreover, the BRD(L) tumor in mice was not able to grow as much as the BRD(H) tumor, and ROI signal of BRD(h) tumor was only 18.08% of BRD(L) on day 28 after the ionizing radiation treatment (Figure 9(C,D)). Tumor

volumes were also measured with calipers following the day of imaging by IVIS (for 28 days) and showed the same pattern as the total flux signal measurement (Figure 9(D)). Similar to the ROI signal pattern, the BRD(L) and BRD(H) implanted mice showed 40.03% and 10.87% tumor volume compared to the control cell implanted mice. Moreover, the BRD(L) tumor in mice was not able to grow as much as the BRD(H) tumor in mice, as only 27.16% of tumor volume was seen on day 28 after the ionizing radiation treatment (Figure 9(E)). Thus, these observations indicate that BRG1-BRD overexpression in HT29 cells exhibits *in vivo* radio-sensitizing efficacy and the radio-sensitizing effect varies depending on the BRG1-BRD overexpression level.

(A)

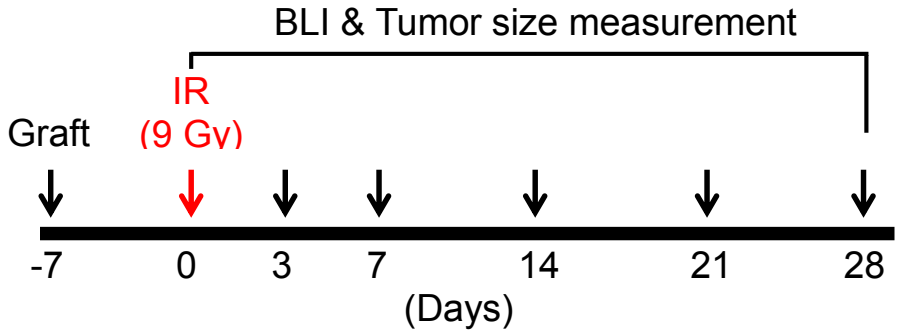
BLI & Tumor size measurement
IR
(9 Gy)
Graft
-7
0
3
7
14
21
28
(Days)

(B)

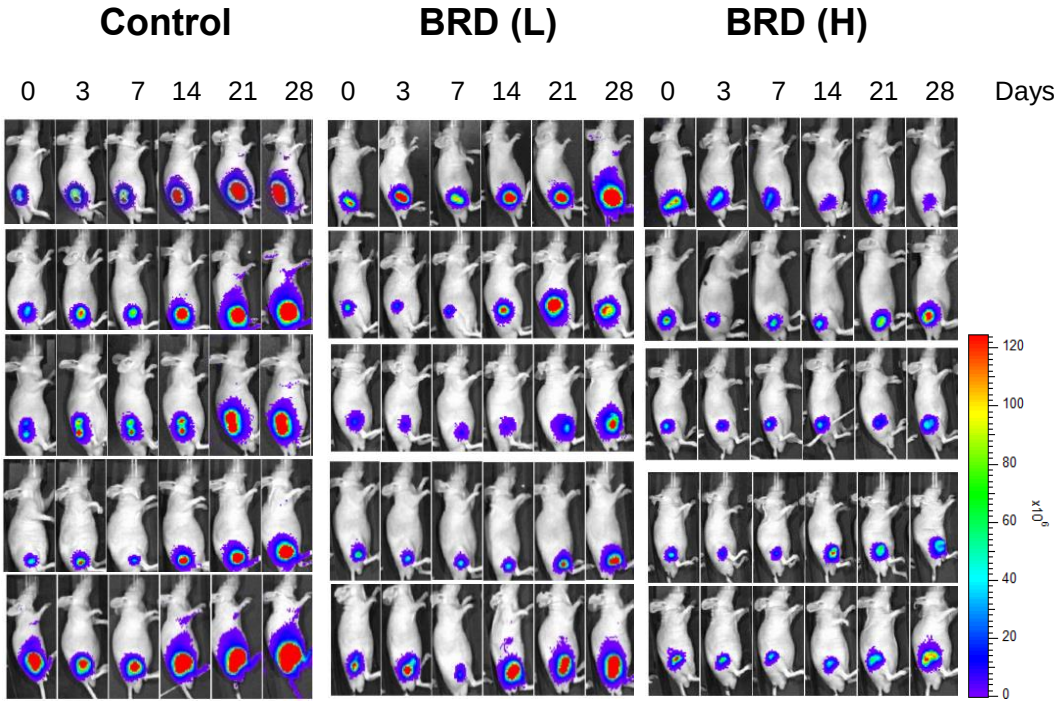
Control
BRD (L)
BRD (H)
0 3 7 14 21 28 0 3 7 14 21 28 0 3 7 14 21 28 Days
120
100
80
60
40
20
0
x10⁶

(C)

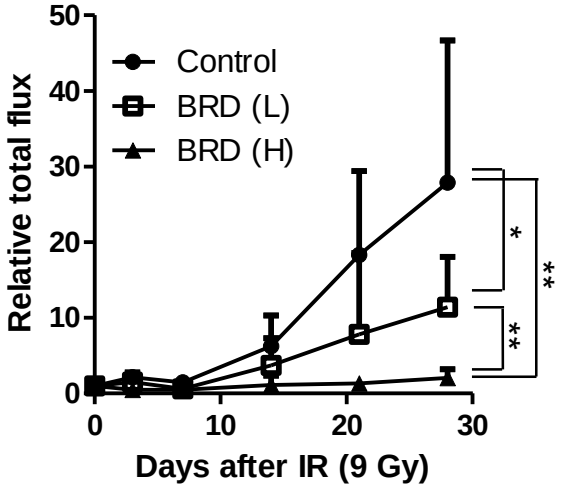
Relative total flux
50
40
30
20
10
0
Control
BRD (L)
BRD (H)
*
**
**
0
10
20
30
Days after IR (9 Gy)

(D)

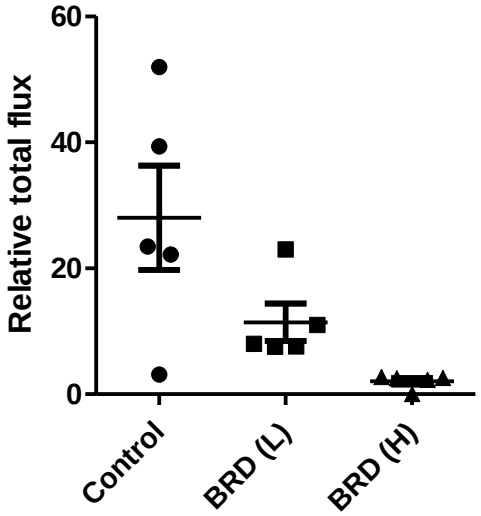
Relative total flux
60
40
20
0
Control
BRD (L)
BRD (H)

(E)

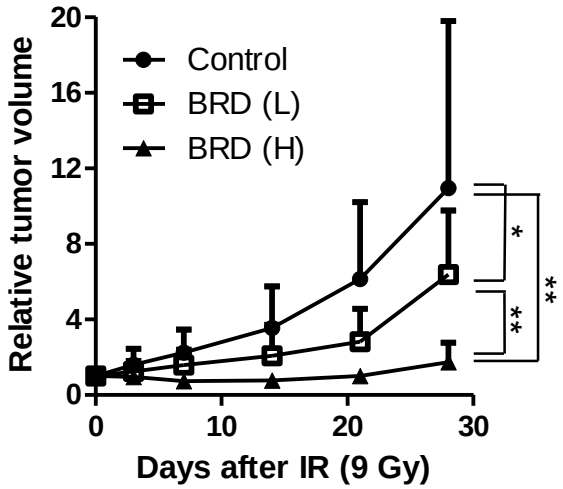
Relative tumor volume
20
16
12
8
4
0
Control
BRD (L)
BRD (H)
*
**
**
0
10
20
30
Days after IR (9 Gy)

(F)

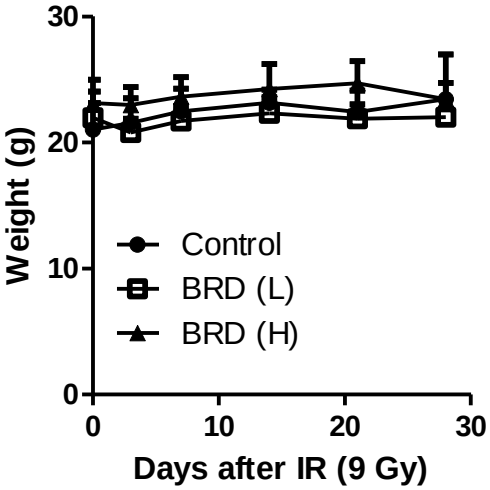
Weight (g)
30
20
10
0
Control
BRD (L)
BRD (H)
0
10
20
30
Days after IR (9 Gy)

Figure 9. Imaging inefficient tumor cell growth with BRG1-BRD overexpression after exposure to external radiation *in vivo.*

(A) A schematic representation of the animal experimental plan. Control, BRD(L), and BRD(H) cells were subcutaneously injected into the flank of Balb/c-nude mice. These mice were then subjected to high energy X-ray irradiation by LINAC. This day was designated as 'day 0' indicating the day of irradiation. These mice were imaged by a bioluminescence imaging modality, measured with calipers, and followed up for 28 days. (B) The bioluminescence images of nude mice with subcutaneous implantation of HT29 cells that were stably transfected with the pMX-BRD vector. (C) Luciferase expression showing the total flux after irradiation was calculated and graphed. (D) A scatter plot on day 28 after irradiation was re-graphed from (C). (E) Tumor volumes were measured and graphed. (F) Mice weights were not found to be significantly related.

Control, filled circles; BRD(L), open squares; BRD(H), filled triangles.

DNA damage after ionizing radiation treatment in high BRG1-BRD overexpressing cells is retained and affects cell proliferation semi-permanently

To investigate whether the residual effect of BRD(L) and BRD(H) in tumors is different or not, the tumor-bearing mice were sacrificed to extract the tumor tissue and these tissues were used to confirm their proliferation rate and residual DNA damage at 30 days after the radiation treatment. Firstly, as the BRD(L) and BRD(H) cells were transfected with BRG1-BRD gene including the myc-tag, the extracted tissues were subjected to immunohistochemistry to check whether the BRG1-BRD overexpression was stably retained. BRD(L) and BRD(H) tumors showed a positively higher mean intensity of the myc-tag than the control (1.80 and 1.78 times each, Figure 10). To confirm the DNA damage retained, the γ-H2AX signal in the BRD(L) tumor was analyzed and the result was similar to that in the control tumor (1.05 times). However, the γ-H2AX signal in the BRD(H) tumor was higher than that in BRD(L) (1.38 times, Figure 10(B)). In order to assess the influence of the residual DNA damage, the cells in the tissues were subjected to binding with the anti-Ki67 antibody, a proliferation marker. The

proliferation rate was sequentially decreased from the Control, BRD(L), and BRD(H), indicating that the residual DNA damage still affected the cell proliferation rate. Moreover, if BRG1-BRD overexpression is high in HT29 cells, their growth is critically disturbed (51.99% lower proliferation of control) after radiation treatment (Figure 10). Similar experiments were conducted with a TUNEL assay in the same tissues. TUNEL assay showed the presence of apoptosis and the percentage of cells undergoing apoptosis was 1.43 times and 2.41 times in BRD(L) and BRD(H) in the TUNEL stained cells compared to the control (Figure 10). This finding indicates that high expression of BRG1-BRD enhances the residual DNA damage and that this damage affects the cell proliferation rate after radiation treatment. In addition, this residual DNA damage induces apoptosis heavily after the radiation treatment.

(A)

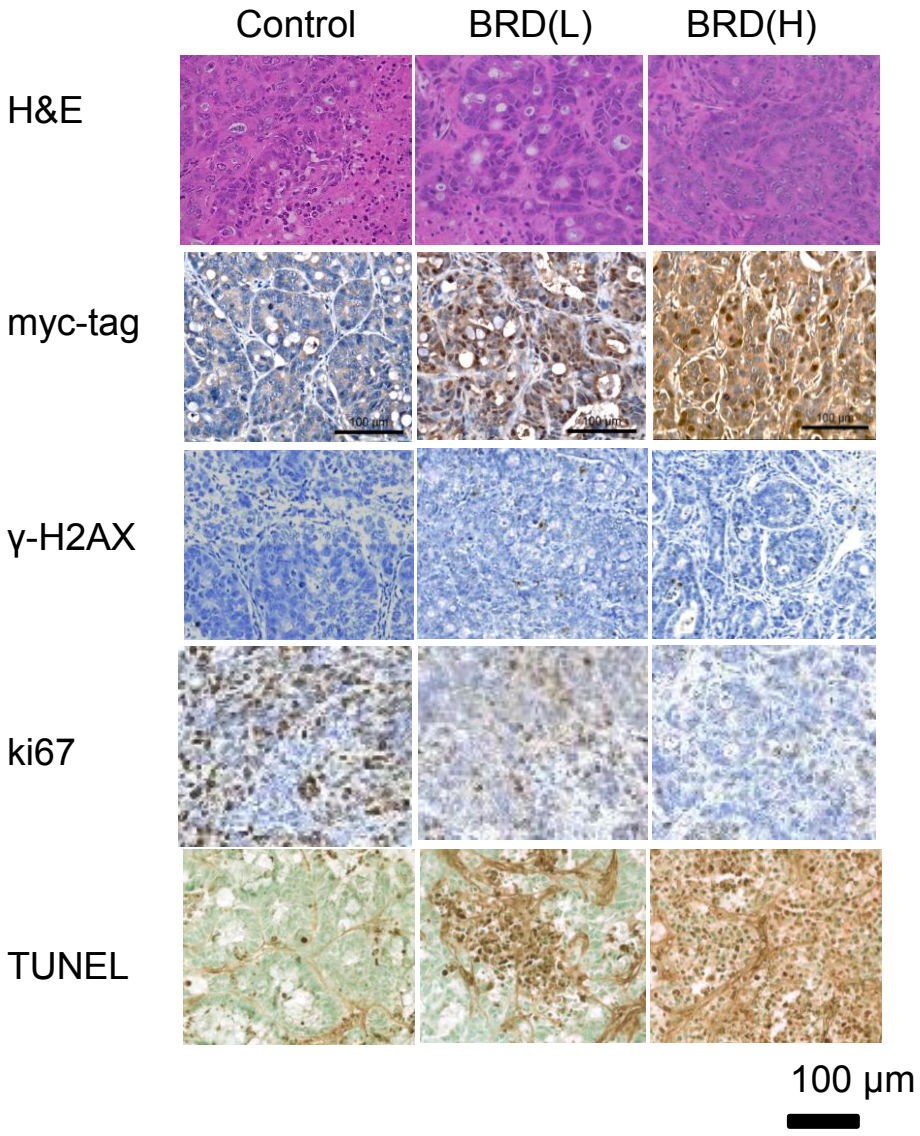

(B)

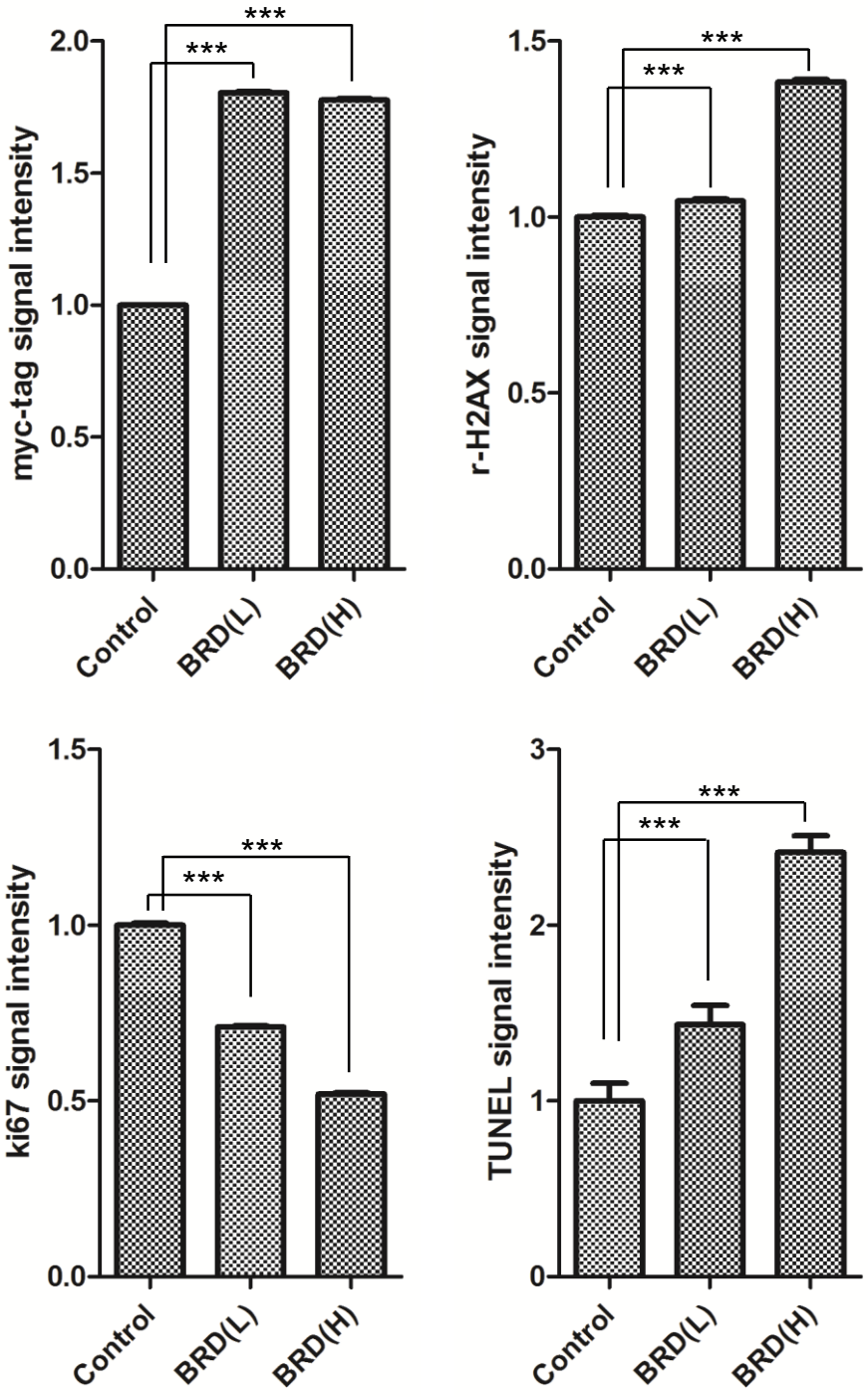
myc-tag signal intensity
2.0
1.5
1.0
0.5
0.0
***
***
Control
BRD(L)
BRD(H)
r-H2AX signal intensity
1.5
1.0
0.5
0.0
***
***
Control
BRD(L)
BRD(H)
ki67 signal intensity
1.5
1.0
0.5
0.0
***
***
Control
BRD(L)
BRD(H)
TUNEL signal intensity
3
2
1
0
***
***
Control
BRD(L)
BRD(H)

Figure 10. Immunohistochemistry of myc-tag, phosphorylated H2AX, and ki67 staining in subcutaneous xenografts from irradiated mice inoculated with BRG1-BRD-overexpressing HT29 cells.

(A) Tumor sections were stained with antibodies specific for myc-tag, phosphorylated H2AX, and ki67 as described in the "Materials and Methods" section. Magnification 200×, scale bar=100 μm. Average DAB intensity and proportion of staining for myc-tag, phosphorylated H2AX, and ki67 in the xenografts was standardized to a negative control. (B) Quantification was derived from the TissueFAXS software quantification analysis. Significant intergroup variations are indicated by *$p < 0.05$, **$p < 0.01$, and ***$p < 0.001$.

Induction of p21 by p53 following DNA damage was boosted by BRG1-BRD overexpression after radiation treatment

In mammalian cells BRG1 is known to play a role in regulating cellular proliferation [35, 36], and the temporally ordered association of BRG1 with histone deacetylase and the retinoblastoma tumor suppressor gene product complex ensures the sequential activation of cyclin E and cyclin A, and maintains the order of the G1 and S phases in the cell cycle [37]. Moreover, G1 phase arrest can be caused by DNA damage, which can activate the p53-p21 pathway [38-45]. In our previous study, we have shown G1 phase arrest with BRG1-BRD overexpression after radiation treatment [46]. Therefore, the status of the p53-p21 pathway under high BRG1-BRD overexpression was an unclear area that needed investigation. Usually, BRG1-containing complexes upregulate p21 expression, which is related to flat cells, growth arrest, and cell senescence [47, 48]. However, BRD(H) which show high BRG1-BRD overexpression show a different pattern compared to control and BRD(L), where BRD(L) shows no difference compared to control, when we confirmed the expression of p53 and p21 (Figure 11).

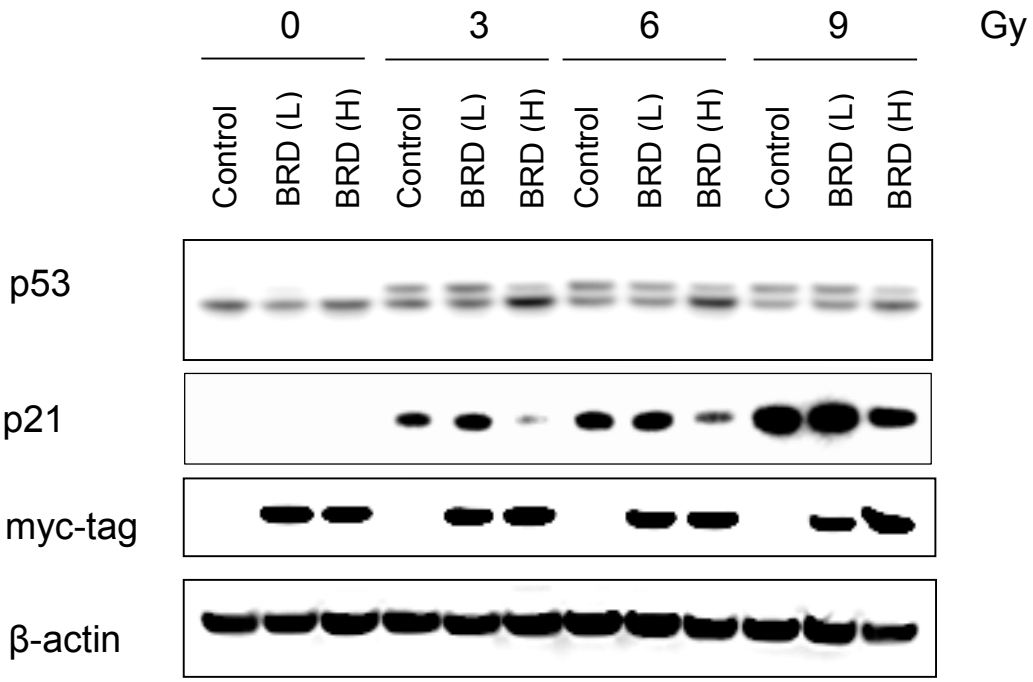

Figure 11. Increased p53 and decreased p21 protein levels with BRG1-BRD overexpression after exposure to external radiation. Lysates from control, BRD(L), and BRD(H) cells that were untreated or treated with ionizing radiation (3, 6, or 9 Gy), were subjected to SDS-PAGE and analyzed by western blotting using anti-p53 or anti-p21 monoclonal antibodies.

DNA repair related genes are downregulated in high BRG1-BRD overexpressing cells after ionizing radiation treatment

We next examined whether other DNA repair related genes were affected by BRG1-BRD overexpression after radiation treatment or whether fragmentary differences exist. Genes are divided into many categories including aging, angiogenesis, apoptotic processes, cell cycle, cell death, cell differentiation, cell migration, cell proliferation, DNA repair, extracellular matrix, immune response, inflammatory response, neurogenesis, RNA splicing, and secretion. All these categories were examined and more than 30,000 genes were included in these categories. Interestingly, the biggest downregulation was observed in DNA repair genes, especially in *SPATA22*, *CDC148*, *MUM1*, *ZRANB3*, *PARP3*, *CHRNA4*, *RAD9B*, and *RAD21L1* (Figure 12(A)). This result suggests that BRG1-BRD overexpression induces the downregulation of genes related to DNA repair after radiation treatment. Moreover, irradiated BRG1-BRD overexpressing cells showed upregulation of genes related to aging, angiogenesis, extracellular matrix, and inflammatory response, and they also showed downregulation of genes related to apoptotic processes, cell cycle, and DNA repair (Figure 12(B-D)). We also examined

p53, p-p53, p21, and CDK2 protein expression after radiation. When BRG1-BRD was overexpressed, p53 and phosphorylated p53 increased evidently after exposure to radiation (Figure 13). DNA damage is known for activating p53 expression through a phosphorylation-acetylation cascade [49]. There is also a report explaining the relationship between p21, p53, and CDK2 activities [38]. Even though DNA damage often activates the p53-p21 pathway leading to CDK2 inhibition, this phenomenon was not observed in this experiment, which indicates that tumor regression due to BRG1-BRD overexpression and external radiation therapy does not follow the p53-p21 pathway alone.

(A)

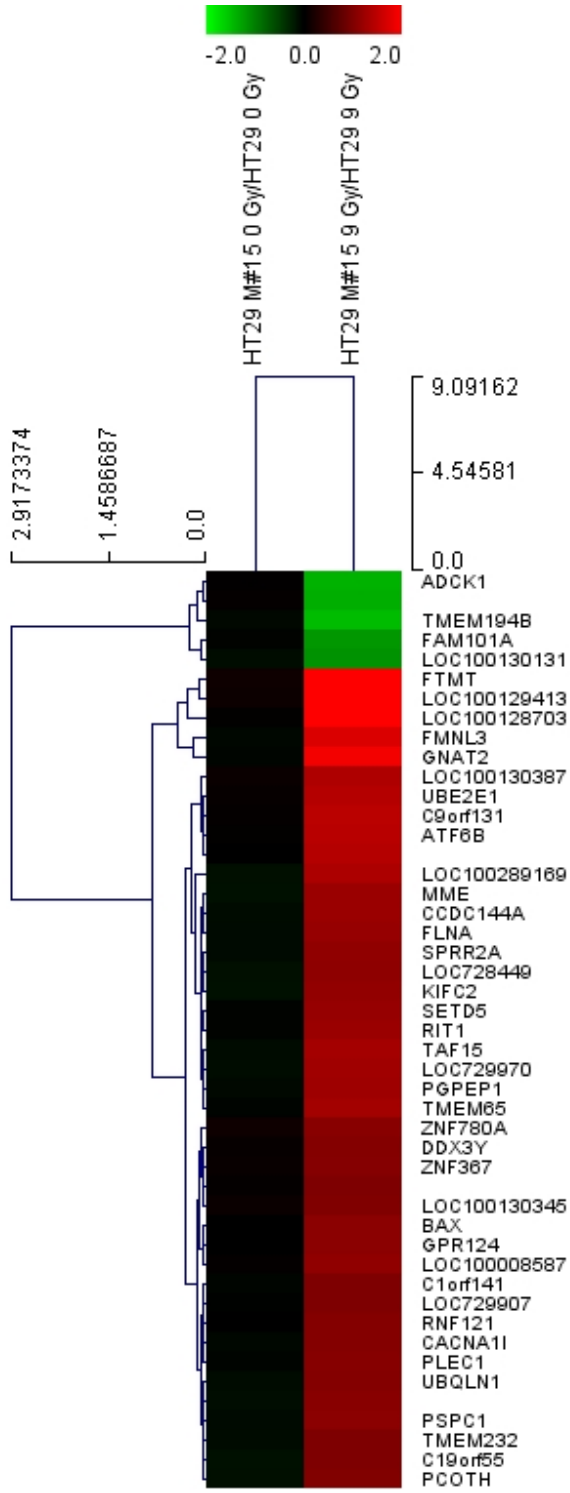
-2.0
0.0
2.0
HT29 M#15 0 Gy/HT29 0 Gy
HT29 M#15 9 Gy/HT29 9 Gy
9.09162
4.54581
0.0
2.9173374
1.4586687
0.0
ADCK1
TMEM194B
FAM101A
LOC100130131
FTMT
LOC100129413
LOC100128703
FMNL3
GNAT2
LOC100130387
UBE2E1
C9orf131
ATF6B
LOC100289169
MME
CCDC144A
FLNA
SPRR2A
LOC728449
KIFC2
SETD5
RIT1
TAF15
LOC729970
PGPEP1
TMEM65
ZNF780A
DDX3Y
ZNF367
LOC100130345
BAX
GPR124
LOC100008587
C1orf141
LOC729907
RNF121
CACNA1I
PLEC1
UBQLN1
PSPC1
TMEM232
C19orf55
PCOTH

(B)

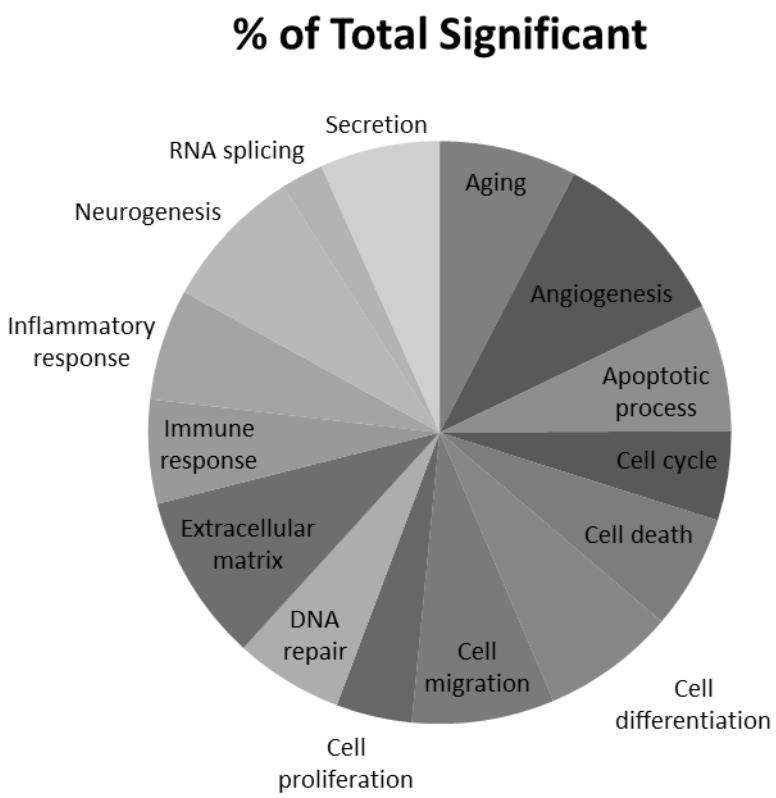
% of Total Significant
Secretion
RNA splicing
Aging
Neurogenesis
Angiogenesis
Inflammatory response
Apoptotic process
Immune response
Cell cycle
Extracellular matrix
Cell death
DNA repair
Cell migration
Cell differentiation
Cell proliferation

(C)

BRD (H) 9 Gy/ Control 9Gy	Significant criteria :		1.5 fold, Flag P			Significant gene filter :										
	Total	Aging	Angiogenesis	Apoptotic process	Cell cycle	Cell death	Cell differentiation	Cell migration	Cell proliferation	DNA repair	Extracellular matrix	Immune response	Inflammatory response	Neurogenesis	RNA splicing	Secretion
Gene Number	7,964	131	140	689	837	855	1,798	380	407	238	200	694	208	844	242	301
% of Total	100.0	1.6	1.8	8.7	10.5	10.7	22.6	4.8	5.1	3.0	2.5	8.7	2.6	10.6	3.0	3.8
Up Significant	402	5	7	16	10	18	55	13	6	0	11	14	8	29	2	7
% of Up Significant	5.0	3.8	5.0	2.3	1.2	2.1	3.1	3.4	1.5	0.0	5.5	2.0	3.8	3.4	0.8	2.3
Dn Significant	151	2	3	18	19	20	38	8	6	10	2	14	1	18	2	7
% of Dn Significant	1.9	1.5	2.1	2.6	2.3	2.3	2.1	2.1	1.5	4.2	1.0	2.0	0.5	2.1	0.8	2.3
Total Significant	**553**	**7**	**10**	**34**	**29**	**38**	**93**	**21**	**12**	**10**	**13**	**28**	**9**	**47**	**4**	**14**
% of Total Significant	6.9	5.3	7.1	4.9	3.5	4.4	5.2	5.5	2.9	4.2	6.5	4.0	4.3	5.6	1.7	4.7

(D)

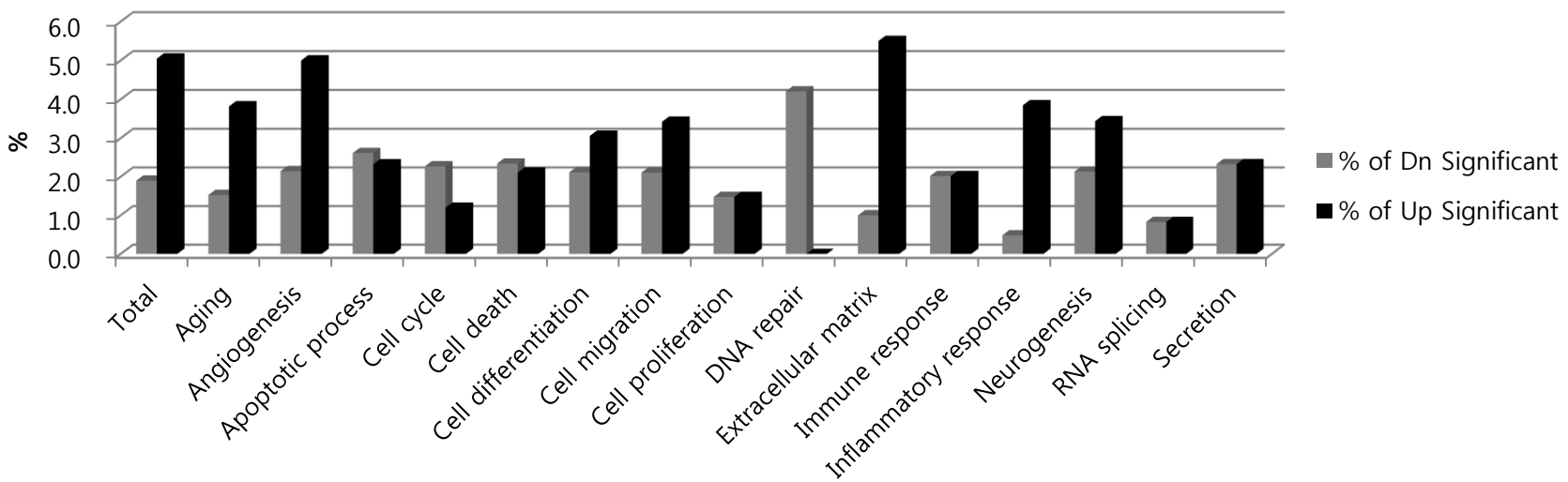

Figure 12. Microarray analysis of BRG1-BRD-overexpressed cells after exposure to external radiation.

(A) Genes downregulated and upregulated after radiation with BRG1-BRD overexpression are shown in the gene tree. (B) Genes showing significantly different expression are sorted by several categories. (C) Details of genes with altered expression from each category are shown in the table. (D) Details of genes showing altered expression from each category are shown on the graph.

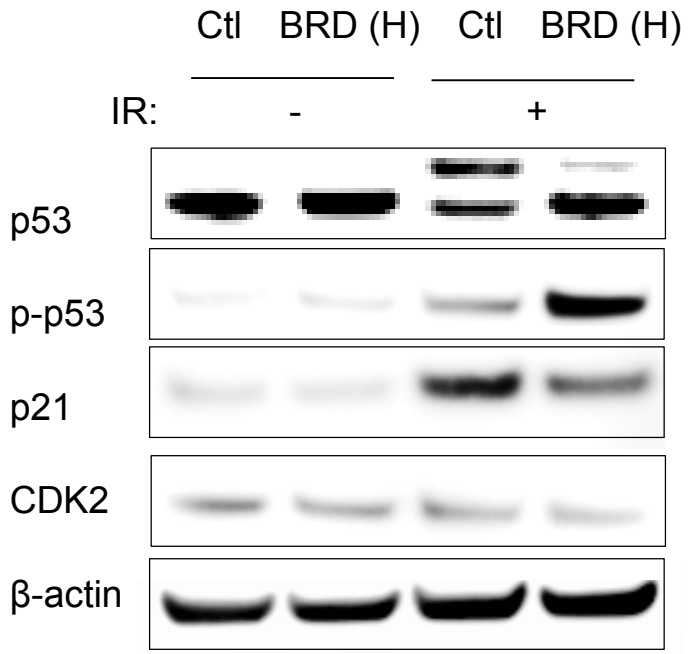

Figure 13. Phosphorylated p53 increases with BRG1-BRD overexpression when exposure to radiation.

Lysates from control and BRD(H) cells, untreated or treated (9 Gy) with ionizing radiation, were subjected to SDS-PAGE and analyzed by western blotting with anti-p-p53 or CDK2 monoclonal antibodies.

DISCUSSION

Radiotherapy has been continuously improved with advances of new instruments and methods. However, general radiotherapy induces several side effects [50-52] and external radiation therapy can be adopted for cancers which are localized or with few metastatic foci. Development of radiosensitizers for the effective killing of tumor cells during radiation therapy is therefore necessary. Blockage in DSB repair by BRG1-BRD overexpression can be adopted as a mechanism for effective radiation therapy [18, 46].

In the present study, sustained damage depending on BRG1-BRD expression levels in a human colon cancer cell line was observed. The level of BRG1-BRD overexpression was evaluated by myc-tag expression. Because the vector included BRD-nuclear localization signals (x3)-myc-tag as inserts. Previously, we proved that BRG1-BRD overexpression shown by myc-tag expression directly regulates chromatin binding level of BRG1 [46]. *In vitro* data such as clonogenic assays and γ-H2AX foci staining showed that high BRG1-BRD overexpression helps in sustaining semi-permanent DNA damage, reducing survival, and

disabled DNA repair. Some reports showed that kinetics of γ−H2AX formation and it matches to the control cell kinetics of γ−H2AX formation [21, 22]. Loss of γ−H2AX was started 8 h after treatment in control cells. However, γ−H2AX expression was increased in BRD(L) and BRD(H) cells.

Furthermore, the BRG1−BRD overexpressing tumor cells grafted in the flank showed slower proliferation than the control. BRD(H)−bearing mice showed 5.56−times slower tumor proliferation than BRD(L) mice on day 28 after radiation treatment. Previously my laboratory proved that BRG1−BRD overexpression increased sensitivity to radiotherapy [46].

One limitation of the present study is which cell lines were used as negative control. A true negative control should be cells transfected with mock vector, the same viral vector without BRD. However, the negative control in this present study was the original cancer cells without transfection of these vector system. The reason was that I failed to establish mock vector. Future studies will be required to transfect mock vector into cells to use them as control. Remaining DNA damage and DNA elimination are important areas of study[8, 9, 53−55], so tissues after radiotherapy were acquired through sacrificing tumor−bearing

mice and the remaining semi-permanent DNA damage in extracted tumor tissue was studied. This study of the BRD(H) revealed that high BRG1-BRD overexpression induces DNA damage which triggers stable apoptosis and this is proven by tissueFAXS quantification [56]. Even though the γ-H2AX assay showed an insignificant increase (1.38 times) after high BRG1-BRD overexpression, the residual DNA damage affects cell proliferation, decreasing it to half of that in the control cells. This seems to result in a 'butterfly effect' where almost all of DNA damaged-vulnerable cells are induced to enter the apoptotic pathway. Apoptosis occurred in 47.94% of the total area in high BRG1-BRD overexpression and low BRG1-BRD overexpressing cells showed a 27.77% apoptosis area. Under normal conditions, DNA self-repair mechanisms are in place, but these mechanisms easily fail when exposed to high BRG1-BRD overexpression leading to irreversible apoptosis. This is the first study to show that the degree of irradiated tumor cell damage is dependent on the level of BRG1-BRD overexpression, highlighting the importance of copy number variation, which accounts for a substantial amount of genetic variation [57]. Moreover, the expression of DNA repair related genes such as

SPATA22, *CDC148*, *MUM1*, *ZRANB3*, *PARP3*, *CHRNA4*, *RAD9B*, and *RAD21L1* was downregulated after radiation treatment. DNA repair-related gene expression after treatment with various doses of radiation is variable and some representative DNA repair-related genes include *CDKN1A*, *ATM*, *RAD50*, *PLK3*, *GADD45A*, *DDB2*, *BBC3*, and *IER5* [58]. Some of these genes, which regulate DNA repair, affect each other but some do not, implying that irradiated BRG1-BRD overexpressed cells may be affected by a different damage pathway. Following the result of the cDNA microarray, the BCL-2 apoptosis pathway [59-62] was shown to directly regulate the death of BRG1-BRD overexpressing cells.

DNA self-repair mechanism after radiation therapy choose homologous recombination (HR) or non-homologous end joining (NHEJ) repair pathway [63-66]. There are several studies indicating the relationship among SWI/SNF complex, K14H3, S139 of H2AX and their role in DNA damage repair [67-69]. Many factors modulating DNA repair pathway such as GCN5, ATM, ATR, DNA-PKcs, CBP/P300, and so on have their own function [70]. This could increase, decrease, or maintain the expression of specific genes that effect to choose one repair

pathway [67]. It seems that DNA self-repair mechanism in this study choose both HR and NHEJ. However, DNA repair pathway related to ATM kinase activation is HR [71, 72]. So, the major DNA repair pathway will be HR.

Nowadays, the majority of gene therapy for clinical trials have exploited viral vectors because they are very efficient vehicles to deliver nucleic acid [73]. Most oncolytic viruses have been engineered from adenovirus or HSV for cancer gene therapy [74]. However, these viral gene therapies can trigger problems of immunological defenses, specificity of transgene delivery, and insertional mutagenesis [74]. Safety of these therapeutic effect is the most important factor to consider. A patient who got virus therapy, Jesse Gelsinger, was dead in a clinical trial for gene therapy in 1999. These disadvantages are challenges to manipulate the proper adoption of BRG1-BRD gene therapy in the future. There are recent studies suggesting the development of gene therapy with oncolytic virus [75-79] by engineering oncolytic viruses for additional benefits from cytokine expression for cancer immune therapy [80]. It is important that developing delivery methodology. Also, recent FDA approval of oncolytic viruses are supportive for their use[81].

In summary, this study revealed a potential therapeutic method using the overexpression of BRG1-BRD as a radiosensitizer. Its competitive inhibition of acetylated H3 K14 blocks DNA self-repair mechanism, which induces effective cancer cell death by radiation.

REFERENCE

1. Connell, P.P., and Hellman, S. (2009). Advances in radiotherapy and implications for the next century: a historical perspective. Cancer research *69*, 383-392.

2. Lanni, T.B., Jr., Grills, I.S., Kestin, L.L., and Robertson, J.M. (2011). Stereotactic radiotherapy reduces treatment cost while improving overall survival and local control over standard fractionated radiation therapy for medically inoperable non-small-cell lung cancer. American journal of clinical oncology *34*, 494-498.

3. DeWeese, T.L. (2004). Radiation therapy and androgen suppression as treatment for clinically localized prostate cancer: the new standard? Jama *292*, 864-866.

4. Niewald, M., Tkocz, H.J., Abel, U., Scheib, T., Walter, K., Nieder, C., Schnabel, K., Berberich, W., Kubale, R., and Fuchs, M. (1996). Rapid course radiation therapy vs. more standard treatment: a randomized trial for bone metastases. International journal of radiation oncology, biology, physics *36*, 1085-1089.

5. Graham, W.J., and Murphy, D.P. (1991). Principles of oncology: how radiation therapy works. The Journal of the Oklahoma State Medical Association *84*, 451-454.

6. Harwood, A.R. (1986). General principles of radiation oncology. The Journal of the Louisiana State Medical Society : official organ of the Louisiana State Medical Society *138*, 19-22.

7. Watanabe, T., Itabashi, M., Shimada, Y., Tanaka, S., Ito, Y., Ajioka, Y., Hamaguchi, T., Hyodo, I., Igarashi, M., Ishida, H., et al. (2012). Japanese Society for Cancer of the Colon and Rectum (JSCCR) guidelines 2010 for the treatment of colorectal cancer. International journal of clinical oncology *17*, 1-29.

8. Roos, W.P., and Kaina, B. (2006). DNA damage-induced cell death by apoptosis. Trends in molecular medicine *12*, 440-450.

9. Roos, W.P., and Kaina, B. (2013). DNA damage-induced cell death: from specific DNA lesions to the DNA damage response and apoptosis. Cancer letters *332*, 237-248.

10. Parisi, A., and Antoine, A.D. (1974). Increased radiation

resistance of vegetative Bacillus pumilus. Applied microbiology *28*, 41-46.

11. Lobrich, M., and Jeggo, P.A. (2007). The impact of a negligent G2/M checkpoint on genomic instability and cancer induction. Nature reviews. Cancer *7*, 861-869.

12. Caldecott, K.W. (2008). Single-strand break repair and genetic disease. Nature reviews. Genetics *9*, 619-631.

13. Demple, B., and DeMott, M.S. (2002). Dynamics and diversions in base excision DNA repair of oxidized abasic lesions. Oncogene *21*, 8926-8934.

14. Hegde, M.L., Hazra, T.K., and Mitra, S. (2008). Early steps in the DNA base excision/single-strand interruption repair pathway in mammalian cells. Cell research *18*, 27-47.

15. Pogozelski, W.K., and Tullius, T.D. (1998). Oxidative Strand Scission of Nucleic Acids: Routes Initiated by Hydrogen Abstraction from the Sugar Moiety. Chemical reviews *98*, 1089-1108.

16. Lewanski, C.R., and Gullick, W.J. (2001). Radiotherapy and cellular signalling. The Lancet. Oncology *2*, 366-370.

17. Ooi, L., Belyaev, N.D., Miyake, K., Wood, I.C., and Buckley, N.J. (2006). BRG1 chromatin remodeling activity is required for efficient chromatin binding by repressor element 1-silencing transcription factor (REST) and facilitates REST-mediated repression. The Journal of biological chemistry *281*, 38974-38980.

18. Lee, S.K., Park, E.J., Lee, H.S., Lee, Y.S., and Kwon, J. (2012). Genome-wide screen of human bromodomain-containing proteins identifies Cecr2 as a novel DNA damage response protein. Molecules and cells *34*, 85-91.

19. Rogakou, E.P., Boon, C., Redon, C., and Bonner, W.M. (1999). Megabase chromatin domains involved in DNA double-strand breaks in vivo. The Journal of cell biology *146*, 905-916.

20. Fernandez-Capetillo, O., Lee, A., Nussenzweig, M., and Nussenzweig, A. (2004). H2AX: the histone guardian of the genome. DNA repair *3*, 959-967.

21. Olive, P.L., and Banath, J.P. (2009). Kinetics of H2AX phosphorylation after exposure to cisplatin. Cytometry. Part B, Clinical cytometry *76*, 79-90.

22. Scarpato, R., Castagna, S., Aliotta, R., Azzara, A., Ghetti, F., Filomeni, E., Giovannini, C., Pirillo, C., Testi, S., Lombardi, S., et al. (2013). Kinetics of nuclear phosphorylation (gamma-H2AX) in human lymphocytes treated in vitro with UVB, bleomycin and mitomycin C. Mutagenesis *28*, 465-473.

23. van Attikum, H., and Gasser, S.M. (2009). Crosstalk between histone modifications during the DNA damage response. Trends in cell biology *19*, 207-217.

24. Lee, H.S., Park, J.H., Kim, S.J., Kwon, S.J., and Kwon, J. (2010). A cooperative activation loop among SWI/SNF, gamma-H2AX and H3 acetylation for DNA double-strand break repair. The EMBO journal *29*, 1434-1445.

25. Hur, S.K., Park, E.J., Han, J.E., Kim, Y.A., Kim, J.D., Kang, D., and Kwon, J. (2010). Roles of human INO80 chromatin remodeling enzyme in DNA replication and chromosome segregation suppress genome instability. Cellular and molecular life sciences : CMLS *67*, 2283-2296.

26. Khafif, A., Hurst, R., Kyker, K., Fliss, D.M., Gil, Z., and Medina, J.E. (2005). Curcumin: a new radio-sensitizer of squamous cell carcinoma cells. Otolaryngology--head and neck surgery : official journal of American Academy of Otolaryngology-Head and Neck Surgery *132*, 317-321.

27. Institute of Laboratory Animal Resources (U.S.). Committee on Care and Use of Laboratory Animals. Guide for the care and use of laboratory animals. In NIH publication. (Bethesda, Md.: U.S. Dept. of Health and Human Services, Public Health Service), p. v.

28. Munro, S., and Pelham, H.R.B. (1984). Use of Peptide Tagging to Detect Proteins Expressed from Cloned Genes - Deletion Mapping Functional Domains of Drosophila Hsp70. Embo Journal *3*, 3087-3093.

29. Franken, N.A., Rodermond, H.M., Stap, J., Haveman, J., and van Bree, C. (2006). Clonogenic assay of cells in vitro. Nature protocols *1*, 2315-2319.

30. Brown, J.M., and Attardi, L.D. (2005). The role of apoptosis in

cancer development and treatment response. Nature reviews. Cancer *5*, 231-237.

31. Podhorecka, M., Skladanowski, A., and Bozko, P. (2010). H2AX Phosphorylation: Its Role in DNA Damage Response and Cancer Therapy. Journal of nucleic acids *2010*.

32. Mah, L.J., El-Osta, A., and Karagiannis, T.C. (2010). gammaH2AX: a sensitive molecular marker of DNA damage and repair. Leukemia *24*, 679-686.

33. Turinetto, V., and Giachino, C. (2015). Multiple facets of histone variant H2AX: a DNA double-strand-break marker with several biological functions. Nucleic acids research *43*, 2489-2498.

34. Laguens, R.P., Meckert, P.M., Martino, J.S., Perrone, S., and Favaloro, R. (1996). Identification of programmed cell death (apoptosis) in situ by means of specific labeling of nuclear DNA fragments in heart biopsy samples during acute rejection episodes. The Journal of heart and lung transplantation : the official publication of the International Society for Heart Transplantation *15*, 911-918.

35. Dunaief, J.L., Strober, B.E., Guha, S., Khavari, P.A., Alin, K., Luban, J., Begemann, M., Crabtree, G.R., and Goff, S.P. (1994). The retinoblastoma protein and BRG1 form a complex and cooperate to induce cell cycle arrest. Cell *79*, 119-130.

36. Strober, B.E., Dunaief, J.L., Guha, S., and Goff, S.P. (1996). Functional interactions between the hBRM/hBRG1 transcriptional activators and the pRB family of proteins. Molecular and cellular biology *16*, 1576-1583.

37. Zhang, H.S., Gavin, M., Dahiya, A., Postigo, A.A., Ma, D.D., Luo, R.X., Harbour, J.W., and Dean, D.C. (2000). Exit from G1 and S phase of the cell cycle is regulated by repressor complexes containing HDAC-Rb-hSWI/SNF and Rb-hSWI/SNF. Cell *101*, 79-89.

38. He, G., Siddik, Z.H., Huang, Z., Wang, R., Koomen, J., Kobayashi, R., Khokhar, A.R., and Kuang, J. (2005). Induction of p21 by p53 following DNA damage inhibits both Cdk4 and Cdk2 activities. Oncogene *24*, 2929-2943.

39. Mytych, J., Zebrowski, J., Lewinska, A., and Wnuk, M. (2016). Prolonged Effects of Silver Nanoparticles on p53/p21 Pathway-

Mediated Proliferation, DNA Damage Response, and Methylation Parameters in HT22 Hippocampal Neuronal Cells. Molecular neurobiology.

40. Dolan, D.W., Zupanic, A., Nelson, G., Hall, P., Miwa, S., Kirkwood, T.B., and Shanley, D.P. (2015). Integrated Stochastic Model of DNA Damage Repair by Non-homologous End Joining and p53/p21-Mediated Early Senescence Signalling. PLoS computational biology *11*, e1004246.

41. Ninomiya, Y., Cui, X., Yasuda, T., Wang, B., Yu, D., Sekine-Suzuki, E., and Nenoi, M. (2014). Arsenite induces premature senescence via p53/p21 pathway as a result of DNA damage in human malignant glioblastoma cells. BMB reports *47*, 575-580.

42. Insinga, A., Cicalese, A., Faretta, M., Gallo, B., Albano, L., Ronzoni, S., Furia, L., Viale, A., and Pelicci, P.G. (2013). DNA damage in stem cells activates p21, inhibits p53, and induces symmetric self-renewing divisions. Proceedings of the National Academy of Sciences of the United States of America *110*, 3931-3936.

43. Chang, L.J., and Eastman, A. (2012). Differential regulation of p21 (waf1) protein half-life by DNA damage and Nutlin-3 in p53 wild-type tumors and its therapeutic implications. Cancer biology & therapy *13*, 1047-1057.

44. Graham, K., Moran-Jones, K., Sansom, O.J., Brunton, V.G., and Frame, M.C. (2011). FAK deletion promotes p53-mediated induction of p21, DNA-damage responses and radio-resistance in advanced squamous cancer cells. PloS one *6*, e27806.

45. Koike, M., Yutoku, Y., and Koike, A. (2011). Accumulation of p21 proteins at DNA damage sites independent of p53 and core NHEJ factors following irradiation. Biochemical and biophysical research communications *412*, 39-43.

46. Kwon, S.J., Lee, S.K., Na, J., Lee, S.A., Lee, H.S., Park, J.H., Chung, J.K., Youn, H., and Kwon, J. (2015). Targeting BRG1 Chromatin Remodeler via Its Bromodomain for Enhanced Tumor Cell Radiosensitivity In Vitro and In Vivo. Molecular cancer therapeutics *14*, 597-607.

47. Hendricks, K.B., Shanahan, F., and Lees, E. (2004). Role for BRG1 in cell cycle control and tumor suppression. Molecular and cellular biology *24*, 362-376.

48. Kang, H., Cui, K., and Zhao, K. (2004). BRG1 controls the activity of the retinoblastoma protein via regulation of p21CIP1/WAF1/SDI. Molecular and cellular biology *24*, 1188-1199.

49. Sakaguchi, K., Herrera, J.E., Saito, S., Miki, T., Bustin, M., Vassilev, A., Anderson, C.W., and Appella, E. (1998). DNA damage activates p53 through a phosphorylation-acetylation cascade. Genes & development *12*, 2831-2841.

50. Hummerich, J., Werle-Schneider, G., Popanda, O., Celebi, O., Chang-Claude, J., Kropp, S., Mayer, C., Debus, J., Bartsch, H., and Schmezer, P. (2006). Constitutive mRNA expression of DNA repair-related genes as a biomarker for clinical radio-resistance: A pilot study in prostate cancer patients receiving radiotherapy. International journal of radiation biology *82*, 593-604.

51. Darby, S.C., Ewertz, M., McGale, P., Bennet, A.M., Blom-Goldman, U., Bronnum, D., Correa, C., Cutter, D., Gagliardi, G., Gigante, B., et al. (2013). Risk of ischemic heart disease in women after radiotherapy for breast cancer. The New England journal of medicine *368*, 987-998.

52. Brown, P.D., Pugh, S., Laack, N.N., Wefel, J.S., Khuntia, D., Meyers, C., Choucair, A., Fox, S., Suh, J.H., Roberge, D., et al. (2013). Memantine for the prevention of cognitive dysfunction in patients receiving whole-brain radiotherapy: a randomized, double-blind, placebo-controlled trial. Neuro-oncology *15*, 1429-1437.

53. Matt, S., and Hofmann, T.G. (2016). The DNA damage-induced cell death response: a roadmap to kill cancer cells. Cellular and molecular life sciences : CMLS.

54. Vadhavkar, N., Pham, C., Georgescu, W., Deschamps, T., Heuskin, A.C., Tang, J., and Costes, S.V. (2014). Combinatorial DNA damage pairing model based on X-ray-induced foci predicts the dose and LET dependence of cell death in human breast cells. Radiation research *182*, 273-281.

55. Blank, J.L., Liu, X.J., Cosmopoulos, K., Bouck, D.C., Garcia, K., Bernard, H., Tayber, O., Hather, G., Liu, R., Narayanan, U., et al. (2013). Novel DNA damage checkpoints mediating cell death induced by the NEDD8-activating enzyme inhibitor MLN4924. Cancer research *73*, 225-234.

56. Bogusz, A.M., Baxter, R.H., Currie, T., Sinha, P., Sohani, A.R., Kutok, J.L., and Rodig, S.J. (2012). Quantitative immunofluorescence reveals the signature of active B-cell receptor signaling in diffuse large B-cell lymphoma. Clinical cancer research : an official journal of the American Association for Cancer Research *18*, 6122-6135.

57. Freeman, J.L., Perry, G.H., Feuk, L., Redon, R., McCarroll, S.A., Altshuler, D.M., Aburatani, H., Jones, K.W., Tyler-Smith, C., Hurles, M.E., et al. (2006). Copy number variation: new insights in genome diversity. Genome research *16*, 949-961.

58. Li, M.J., Wang, W.W., Chen, S.W., Shen, Q., and Min, R. (2011). Radiation dose effect of DNA repair-related gene expression in mouse white blood cells. Medical science monitor : international medical journal of experimental and clinical research *17*, BR290-297.

59. Chen, D., Zheng, X., Kang, D., Yan, B., Liu, X., Gao, Y., and Zhang, K. (2012). Apoptosis and expression of the Bcl-2 family of proteins and P53 in human pancreatic ductal adenocarcinoma. Medical principles and practice : international journal of the Kuwait University, Health Science Centre *21*, 68-73.

60. Zhang, L., and Zhang, S. (2011). Modulating Bcl-2 family proteins and caspase-3 in induction of apoptosis by paeoniflorin in human cervical cancer cells. Phytotherapy research : PTR *25*, 1551-1557.

61. Ola, M.S., Nawaz, M., and Ahsan, H. (2011). Role of Bcl-2 family proteins and caspases in the regulation of apoptosis. Molecular and cellular biochemistry *351*, 41-58.

62. Oshima, Y., Akiyama, T., Hikita, A., Iwasawa, M., Nagase, Y., Nakamura, M., Wakeyama, H., Kawamura, N., Ikeda, T., Chung, U.I., et al. (2008). Pivotal role of Bcl-2 family proteins in the regulation of chondrocyte apoptosis. The Journal of biological chemistry *283*, 26499-26508.

63. Haines, J.W., Coster, M., and Bouffler, S.D. (2015). Impairment of the non-homologous end joining and homologous recombination pathways of DNA double strand break repair: Impact on spontaneous and radiation-induced mammary and intestinal tumour risk in Apc min/+ mice. DNA repair *35*, 19-26.

64. Moeller, R., Reitz, G., Li, Z., Klein, S., and Nicholson, W.L. (2012). Multifactorial resistance of Bacillus subtilis spores to high-energy proton radiation: role of spore structural components and the homologous recombination and non-homologous end joining DNA repair pathways. Astrobiology *12*, 1069-1077.

65. Takata, M., Sasaki, M.S., Sonoda, E., Morrison, C., Hashimoto, M., Utsumi, H., Yamaguchi-Iwai, Y., Shinohara, A., and Takeda, S. (1998). Homologous recombination and non-homologous end-joining pathways of DNA double-strand break repair have overlapping roles in the maintenance of chromosomal integrity in vertebrate cells. The EMBO journal *17*, 5497-5508.

66. Hunt, C.R., Ramnarain, D., Horikoshi, N., Iyengar, P., Pandita, R.K., Shay, J.W., and Pandita, T.K. (2013). Histone modifications and DNA double-strand break repair after exposure to ionizing radiations. Radiation research *179*, 383-392.

67. Pandita, T.K., Lieberman, H.B., Lim, D.S., Dhar, S., Zheng, W., Taya, Y., and Kastan, M.B. (2000). Ionizing radiation activates the ATM kinase throughout the cell cycle. Oncogene *19*, 1386-1391.

68. Tamburini, B.A., and Tyler, J.K. (2005). Localized histone acetylation and deacetylation triggered by the homologous recombination pathway of double-strand DNA repair. Molecular and cellular biology *25*, 4903-4913.

69. Chai, B., Huang, J., Cairns, B.R., and Laurent, B.C. (2005). Distinct roles for the RSC and Swi/Snf ATP-dependent chromatin remodelers in DNA double-strand break repair. Genes & development *19*, 1656-1661.

70. Ogiwara, H., Ui, A., Otsuka, A., Satoh, H., Yokomi, I., Nakajima, S., Yasui, A., Yokota, J., and Kohno, T. (2011). Histone acetylation by CBP and p300 at double-strand break sites facilitates SWI/SNF chromatin remodeling and the recruitment of non-homologous end joining factors. Oncogene *30*, 2135-2146.

71. Morrison, C., Sonoda, E., Takao, N., Shinohara, A., Yamamoto, K., and Takeda, S. (2000). The controlling role of ATM in homologous recombinational repair of DNA damage. The EMBO journal *19*, 463-471.

72. Beucher, A., Birraux, J., Tchouandong, L., Barton, O., Shibata, A., Conrad, S., Goodarzi, A.A., Krempler, A., Jeggo, P.A., and Lobrich, M. (2009). ATM and Artemis promote homologous recombination

of radiation-induced DNA double-strand breaks in G2. The EMBO journal *28*, 3413-3427.

73. Giacca, M., and Zacchigna, S. (2012). Virus-mediated gene delivery for human gene therapy. Journal of controlled release : official journal of the Controlled Release Society *161*, 377-388.

74. Thomas, C.E., Ehrhardt, A., and Kay, M.A. (2003). Progress and problems with the use of viral vectors for gene therapy. Nature Reviews Genetics *4*, 346-358.

75. Chen, X., Han, J., Chu, J., Zhang, L., Zhang, J., Chen, C., Chen, L., Wang, Y., Wang, H., Yi, L., et al. (2016). A combinational therapy of EGFR-CAR NK cells and oncolytic herpes simplex virus 1 for breast cancer brain metastases. Oncotarget.

76. Gong, J., Sachdev, E., Mita, A.C., and Mita, M.M. (2016). Clinical development of reovirus for cancer therapy: An oncolytic virus with immune-mediated antitumor activity. World journal of methodology *6*, 25-42.

77. Cheng, X., Wang, W., Xu, Q., Harper, J., Carroll, D., Galinski, M.S., Suzich, J., and Jin, H. (2016). Genetic Modification of Oncolytic Newcastle Disease Virus for Cancer Therapy. Journal of virology *90*, 5343-5352.

78. Mansfield, D.C., Kyula, J.N., Rosenfelder, N., Chao-Chu, J., Kramer-Marek, G., Khan, A.A., Roulstone, V., McLaughlin, M., Melcher, A.A., Vile, R.G., et al. (2016). Oncolytic vaccinia virus as a vector for therapeutic sodium iodide symporter gene therapy in prostate cancer. Gene therapy *23*, 357-368.

79. Jun, K.H., Gholami, S., Song, T.J., Au, J., Haddad, D., Carson, J., Chen, C.H., Mojica, K., Zanzonico, P., Chen, N.G., et al. (2014). A novel oncolytic viral therapy and imaging technique for gastric cancer using a genetically engineered vaccinia virus carrying the human sodium iodide symporter. Journal of experimental & clinical cancer research : CR *33*, 2.

80. Bourgeois-Daigneault, M.C., Roy, D.G., Falls, T., Twumasi-Boateng, K., St-Germain, L.E., Marguerie, M., Garcia, V., Selman, M., Jennings, V.A., Pettigrew, J., et al. (2016). Oncolytic vesicular stomatitis virus expressing interferon-gamma has enhanced therapeutic activity. Molecular therapy oncolytics *3*, 16001.

81. Ledford, H. (2015). Cancer-fighting viruses win approval. Nature

526, 622-623.

국문 초록

서론: 방사선 민감제는 보다 효과적인 방사선치료를 위하여 필요하다. Brahma-related gene 1 (BRG1)은 SWI/SNF 크로마틴 리모델링 복합체의 촉매소단위로써, DNA 의 두 가닥 파손과 치료에 관여한다. BRG1-브로모도메인이 과발현 되게 되면, BRG1 은 경쟁적 저해 작용에 의하여 파손된 DNA 를 치료하지 못하게 되며, DNA 의 두 가닥 파손은 그대로 남게 된다. 이 연구의 전략은 BRG1-브로모도메인을 DNA 의 두가닥 파손 치료를 방해하는 경쟁자로 도입시키면서 방사선 치료의 효과를 증진시키는 데에 있다.

방법: 암세포의 성장을 영상화 하기 위하여 루시페라아제가 발현하는 세포주를 형성하고 종양의 크기를 캘리퍼로 측정 하였다. 또, IVIS 영상 시스템을 통한 광학 영상을 얻음으로써 종양의 성장을 간접적으로 측정하였다. 외부방사선에 의한 치료효과를 관찰하기 위하여, 실험에는 인체 대장암 세포 주 HT29 를 사용하였다. 레트로바이러스의 pMX-BRG1-브로모도메인 벡터를 사용하여 HT29 세포에 형질전환 시키고 BRG1-브로모도메인의 발현정도를 나누어 BRG1-브로모도메인의 높은 발현을 가진 HT29 세포(BRD(H))와 BRG1-브로모도메인의 낮을 발현을 가진 HT29 세포(BRD(L))로 나누었다. 세슘-137 방사선 조사장치(IBL 437C)를 이용하여 9 그레이의 선량을 세포에 조사하였다. 개발된 방사

선 민감제의 효과는 클론형성분석법 및 γ-H2AX foci 를 통해 유전자 손상 신호를 분석하는 방법으로 평가하였다. 마우스 피하에 이식된 암세포를 분자영상기법으로 정량분석하고 크기를 측정함으로써 생체 내에서의 효과를 평가하였다.

결과: BRD(L)과 BRD(H) 세포에 방사선을 조사한 뒤 세포의 생존률을 각각 측정하였을 때 대조군을 기준으로 51.4%와 2.2%의 생존률을 보였다. 인산화된 H2AX foci 형광의 강도 역시 방사선 조사 뒤에 대조군의 2.9 배(BRD(L))와 9.9 배(BRD(H))였다. 마우스 모델에서 종양의 성장은 BRG1-브로모도메인의 과발현 정도에 따라 성장이 다르게 억제되었다. BRD(L)과 BRD(H)의 세포를 이용하여 형성된 종양을 X 선 치료 후 28 일째에 루시페라아제의 발현을 측정하였다. 그 결과, 대조군에 비하여 BRD(L)의 경우 40.77%(p=0.048), BRD(H)의 경우 7.37%(p=0.018)로 대조군에 비해 감소되었다.

결론: BRG1-브로모도메인의 과발현을 이용한 방사선 민감제를 개발하였다. 특히 인체 대장암 세포를 이용한 외부방사선 조사실험으로 BRG1-브로모도메인의 과발현을 이용한 방사선 민감제 효과를 증명하였고, 방사선 치료의 효율을 높여줄 수 있음을 분자영상기법을 통하여 보여주었다.

주요어 : BRG1-브로모도메인, 방사선 민감제, 효과적 방사선 치료, 경쟁적 저해제, 유전자 과발현, X 선 치료

학 번 : 2010-21902